TAMPERE UNIVERSITY OF TECHNOLOGY

ELHAM MORADI

CHARACTERIZATION OF EMBROIDERED DIPOLE-TYPE RFID TAG ANTENNAS

Master of Science Thesis

Examiners: Prof. Lauri Kettunen and
Adj.Prof. Leena Ukkonen
Department of Electronics
Faculty Council Meeting: 6 June 2012

ABSTRACT

TAMPERE UNIVERSITY OF TECHNOLOGY
Master's Degree Programme in Signal Processing and Communications Engineering

MORADI, ELHAM: CHARACTERIZATION OF EMBROIDERED DIPOLE-TYPE RFID TAG ANTENNAS

Master of Science Thesis, 63 pages
June 2012
Major subject: Electromagnetic Physics
Examiner: Adjunct Professor Leena Ukkonen and Professor Lauri Kettunen
Keywords: UHF RFID, embroidered antenna, conductivity, conductive thread, sewing machine

Radio Frequency Identification (RFID) is a technology which is used for automatic identification of objects. A typical RFID system consists of a stationary radio-scanner unit, called reader, and a movable transponder, called tag, which is attached to an object. The tags include an antenna and a microchip with internal read/write memory.

Tag antenna plays an important role in the overall RFID system performance factors, such as the read range, and the compatibility with tagged objects. This thesis focuses on garment-integrated embroidered tags which can be used for the means of human monitoring and identification. The embroidered tag antennas are sewed on fabric using conductive threads and computer aided sewing machine.

Modeling of embroidered tag antennas is not a straightforward task, because embroidered antennas do not have a distinct conductivity, which could be used in the simulation model of them. In fact, conductivity of sewed flat conductive layer depends on the selection of the conductive thread, the thread and stitch density and the sewing pattern. The aim of this thesis has been to investigate the effect of these factors on the conductivity, and evaluate conductivity values for the embroidered dipole-type RFID tag antennas.

In this project, T-matched dipoles have been sewed on cotton with two different sewing patterns and also with many different stitch densities. The effect of the geometry of the antenna is also investigated by sewing and measuring straight simple dipoles with both sewing patterns. The achieved read range values of the sewed tag antennas have been up to 7.5 m.

In this thesis it is proved that each sewing pattern has its own conductivity and conductivity of a sewing pattern improves if the pattern consists of sewed lines along the direction of current flow. It is not necessary to sew the antenna with a high thread and stitch density. We can achieve high conductivities even from very sparsely sewed antennas, using less conductive threads and spending considerably less time on sewing.

The evaluated conductivities and the presented simulation model of the sewed dipoles in this project can be used in future for optimization of the sewed antennas to operate in the vicinity of body.

PREFACE

This Master of Science's Thesis is conducted in the Department of Electronics, Rauma Research Unit, at Tampere University of Technology.

I would like to thank Professor Lauri Kettunen for his support and guidance during the past years. I am also grateful to Adjunct Professor Leena Ukkonen for giving me the opportunity to work in this research unit, and for her assistance in this project. I would also like to thank M.Sc. Toni Björninen for his helpful comments and suggestions.

My special thanks are reserved to my parents who have supported and encouraged me throughout all my life. My sincerest appreciation goes to my husband for his warm supports, and for helping me whenever I have needed. Without their warm support and encouragement this would have been impossible to achieve.

CONTENTS

SYMBOLS

A_e	Effective aperture [m]
α	Real part of propagation constant, attenuation factor [Np/m]
a	acceleration [m/s^2]
B	Magnetic flux density [Wb/m^2]
β	Imaginary part of propagation constant, phase constant [rad/m]
c	Velocity of light
D	Electric flux density [C/m^2]
D	Directivity of the antenna [dBi]
δ	Skin depth [m]
E	Electric field intensity [V/m]
E_x	x component of the electric field [V/m]
E_y	y component of the electric field [V/m]
E_z	z component of the electric field [V/m]
e	Radiation efficiency
ε	Permittivity of the media [F/m]
ε_0	Permittivity of free space [F/m]
ε_c	complex permittivity of the media [F/m]
ε_r	Relative permittivity of the media
ε'	Real part of complex permittivity [F/m]
ε''	Imaginary part of complex permittivity [F/m]
f	frequency [Hz]
G	Gain of the antenna [dBi]
G_r	Realized gain [dBi]
γ	Propagation constant [m^{-1}]
Γ	Reflection coefficient
H	Magnetic field intensity [A/m]
H_x	x component of the magnetic field [A/m]
H_y	y component of the magnetic field [A/m]
H_z	z component of the magnetic field [A/m]
J	Electric current density [A/m^2]
J_s	Surface current density [A/m^2]
k	Wave number [rad/m]
k_0	Free space wave number [rad/m]
k_c	Complex wave number [rad/m]
L	Cable loss [W]
λ	Wave length [m]
M	Magnetic current density [V/m^2]
μ	Permeability of the media [H/m]
μ_0	Permeability of free space [H/m]
η	Intrinsic impedance of the medium [Ω]

η_0	Intrinsic impedance of free space [Ω]
Ps	Complex electromagnetic power delivered by the sources [W]
P_0	The time-average power leaving the volume V [W]
P_l	The time-average power dissipated in the volume V due to losses [W]
P_r	Power radiated by the antenna [W]
P_{in}	Power supplied to the terminals of the antenna [W]
P_L	Power lost in the antenna [W]
q_v	electric charge density [C/m^3]
q_s	Surface charge density [C/m^2]
q_l	Charge per unit length [C/m]
Qt	total quality factor
Q_r	Quality factor due to radiation losses
Q_c	Quality factor due to conduction (ohmic) losses
Q_d	Quality factor due to dielectric losses, and
Q_{sw}	Quality factor due to surface waves
r	Read range [m]
R	Resistance [Ω]
ρ	Electric charge density [C/m^3]
S	Poynting vector [W/m^2]
σ	Conductivity of the media [S/m]
σ	Radar cross section [m]
τ	Power transfer coefficient
U	Radiation intensity [W/sr]
u	Velocity of electromagnetic wave in media [m/s]
u_p	Phase velocity [m/s]
v	velocity [m/s]
We	Electric energy density [J/m^3]
Wm	Magnetic energy density [J/m^3]
ω	angular frequency [rad/s]
X	Reactance [Ω]
Z	Impedance [Ω]

ABBRIVIATIONS

BANs	Body-Area Networks
EIRP	Effective Isotropic Radiated Power
GPS	Global Positioning System
Hf	High frequency region (13.56 MHz)
IC	Integrated Circuit
LF	Low frequency region (125-134 kHz)
PANs	Personal Area Networks
PDMS	Polydimethylsiloxane, polymer-ceramic composite
RFID	Radio Frequency Identification
UHF	Ultra high frequency region (860-960 MHz)
VSWR	Voltage standing wave ratio
WLAN	Wireless Local Area Network
4G	Fourth generation mobile communication system

1. INTRODUCTION

Radio Frequency Identification (RFID) is a technology which uses RF signals for automatic identification of objects. RFID technology has two distinct advantages over the traditional identification method, bar code. A barcode indicates the type of the object on which it is printed, while RFID tag includes a unique serial number that distinguishes among many millions of identically manufactured objects. Furthermore, bar codes require line-of-sight with reader, and thus careful physical positioning of scanned objects. Bar code scanning also requires human intervention, but RFID tags are readable at rates of hundreds per second without line-of-sight contact, and without precise positioning [1]. The advantages of this technology over traditional identification methods, and also the development of microelectronic technology in the 1970s have led to continuous development of RFID technology [2]. A typical RFID system consists of a stationary radio-scanner unit, called reader, and a movable transponder, called tag, which is attached to an object. The tags include an antenna and a microchip with internal read/write memory.

RFID systems can be classified based on the power source of the tags; active, semi-passive and passive. Active and semi-passive tags require power source, while passive tags provide their energy from a portion of the transmitted RF wave by the reader antenna. In an RFID system, reader tries to read the information stored in the tag microchip by sending an unmodulated signal to the tag. When the tag receives the signal, it reads the stored data in its internal memory, and acts as a switch to match or mismatch its internal load to the antenna in a coded manner corresponding to the stored data. Thus, the tag scatters a modulated signal for the reader. The reader then demodulates and decodes the signal and gives the data stored in the tag as output [2].

Several frequency bands are standardized for RFID technology. Low frequency (LF, 125-134 kHz) RFID systems are used for applications as access control, animal tracking, immobilizers, healthcare applications, and product authentication. High frequency (HF) RFID systems operate at 13.56 MHz. Typical HF applications are smart cards, smart shelves for item level tracking, and are also currently used to track library books, healthcare patients, product authentication and airline baggage. LF and HF RFID systems have relatively short read ranges, because communication happens in the near field of the reader antenna. These systems are based on quasi-static magnetic coupling among the reader's and tag's coils. On the other hand, UHF (860-960 MHz) and microwave (2.4 GHz and 5.8 GHz) systems use electromagnetic interaction among the reader antenna and the tag antenna when the tag is located at the far field of the reader antenna. As a consequence, these systems have longer read ranges. Long read ranges of UHF

systems make possible applications such as electronic toll collection systems on highways, parking lot access and supply chain management.

Tag antenna plays an important role in the overall RFID system performance factors, such as the read range, and the compatibility with tagged objects. This project focuses on the design and modeling of wearable flexible embroidery UHF RFID tag antennas, using sewing machine as the fabrication method. Wearable antennas for WLAN, GPS, and military related applications have been designed and studied in [3], [4], [5], and [6]. But wearable tags are considerably new subject of research. Wearable tags can be applied for youngsters, the aged, athletes and patients for the purpose of monitoring. Like all other wearable antennas, wearable tags should be light weight, low cost, flexible, and almost maintenance-free, and they should not need installation. One of the best wearable tag antenna fabrication techniques could be sewing an antenna on the wearable fabrics, using conductive threads. An embroidery RFID tag can have any shape such as logo of a company, or a letter shape [7]. Consequently, embroidery tags can be unnoticeable and embedded in the fabric, removing the need of installation. Conductive threads used in sewing the tag antenna are also washable and flexible.

Designing an embroidery tag antenna has some challenges. The electrical properties of the fabric used as substrate (in this project, cotton) of the antenna should be determined. In this project we have used the resonance method [8] for determining the relative permittivity and the loss tangent of cotton. In designing an embroidery tag antenna, with electromagnetic simulators, we can treat the complex embroidery pattern as a uniform conductive material layer, when the pattern is sewed densely. Hence, it is the conductivity of an embroidery pattern that is an effective factor in the simulation model of an embroidery antenna. The conductivity of an embroidery pattern depends on the selection of the conductive thread, the thread density and the sewing structure [7] [9] [10] [11]. In this project, we have determined the conductivity of dipole-type UHF RFID tag antennas with various sewing patterns and with different stitch and thread densities.

The thesis first presents the electromagnetic theory, and explains the excitation and propagation of electromagnetic waves in different mediums. Electromagnetic theory is the basis of antenna theory, which is discussed in Chapter 3. In this chapter, different antenna configurations, and the most important antenna parameters are also illustrated. Then, Chapter 4 gives information about RFID systems, and the major components of RFID system. It also presents factors that evaluate the performance of RFID components in detail. This project deals with wearable sewed RFID tag antennas. Chapter 5 discusses about applications and requirements of wearable antennas. This chapter also summarizes different manufacturing techniques of wearable antennas fabricated up to now.

In Chapter 6, the design of a dipole-type tag antenna (made of copper and textile) is explained. Then, in Chapter 7, the geometry and the measurement results of sewed dipoles with different sewing patterns is represented. In this chapter, also the conductivities of sewed structures are determined. Finally, in Chapter 8, there is a conclusion about the achieved results of this project.

2. ELECTROMAGNETIC THEORY

Electromagnetic theory explains the origin and propagation of electromagnetic waves in different materials. Microwaves are electromagnetic waves with frequencies between 300 MHz and 300 GHz, and with corresponding electrical wavelengths between 1 m and 1 mm. In microwave components, the phase of a voltage or current changes significantly over the physical extend of the device, because the device dimensions are of the order of the microwave wavelength. In contrast, in standard circuit theory wavelengths are much longer than the device dimensions. Consequently, microwave network problems cannot be solved by using standard circuit theory, and they are solved using electromagnetic theory which is based on Maxwell's equations. In fact, also circuit theory is based on Maxwell's equations, but it is an approximation of electromagnetic theory [12].

Modern electromagnetic theory was founded when James Clerk Maxwell presented mathematical formulations for propagation of electromagnetic waves in 1873. Maxwell's equations describe how electric charges and electric currents act as sources for the electric and the magnetic fields. Further, they describe how a time varying electric field generates a time varying magnetic field and vice versa. Maxwell's equations were cast in their modern form by Oliver Heaviside, during the period from 1885 to 1887. Heaviside removed many of the mathematical complexities of the Maxwell's theory. He introduced vector notation, and provided a foundation for practical applications of guided waves and transmission lines. Heinrich Hertz, a German professor of physics and a gifted experimentalist, carried out a set of experiments during the period 1887-1891 that completely validated Maxwell's theory of electromagnetic waves [12].

Because of the lack of reliable microwave sources and other microwave components, the growth of radio technology occurred primarily in the high frequency region to very high frequency region in the early 1900s. In 1940s, during World War II microwave theory and technology received substantial interest due to the development of radar. The work done for radar systems were then benefitted in developing communication systems [12].

This chapter will outline the fundamental concepts of electromagnetic theory that will be required for the rest of this project. Hence, this chapter presents Maxwell's equations, and discusses about boundary conditions and the effect of materials. Wave phenomenon is of essential importance in microwave engineering, so in this chapter also the excitation and propagation of electromagnetic waves, especially plane waves, is discussed.

2.1. Maxwell's equations

Maxwell's equations can be presented in two forms; either in differential form or in integral form. The integral forms of Maxwell's equations describe how the sources and varying fields affect the integrals of the fields over a closed surface, or over a closed line. The integral forms of Maxwell's equations are [12]

$$\int_{\partial s} \boldsymbol{H} \cdot \boldsymbol{dl} = \int_{s} \left(\boldsymbol{J} + \frac{\partial \boldsymbol{D}}{\partial t} \right) \cdot \boldsymbol{n}\, da \quad \forall \mathrm{S}, \qquad \text{(Ampère-Maxwell law)} \qquad (2.1)$$

$$\int_{\partial s} \boldsymbol{E} \cdot \boldsymbol{dl} = -\frac{d}{dt} \int_{s} \boldsymbol{B} \cdot \boldsymbol{n}\, da \quad \forall \mathrm{S}, \qquad \text{(Faraday's law)} \qquad (2.2)$$

$$\int_{\partial V} \boldsymbol{B} \cdot \mathbf{n}\, \mathrm{da} = 0 \quad \forall \mathrm{V}, \qquad \text{(Gauss's law for magnetism)} \qquad (2.3)$$

$$\int_{\partial V} \boldsymbol{D} \cdot \mathbf{n}\, \mathrm{da} = \int_{V} \rho\, dV \quad \forall \mathrm{V}, \qquad \text{(Gauss's law)} \qquad (2.4)$$

where **H** is the magnetic field intensity (A/m), **E** is the electric field intensity(V/m), **B** is the magnetic flux density (Wb/m^2), **D** is the electric flux density (C/m^2), ρ is the electric charge density (C/m^3), **J** is the electric current density (A/m^2), S represents surfaces and V volumes in space. The first equation states that a moving electric charge (current) and a time varying electric flux create a magnetic field. The second equation means that a time varying magnetic flux creates an electric field. Equation (2.3) states that magnetic flux lines are closed, in other words magnetic charges do not exist. The last equation states that the electric charge distribution 'imposes' the electric field [13 p. 20].

The differential forms of Maxwell's equations represent the electric and magnetic fields locally. The differential forms of Maxwell's equations can be expressed as [14 p. 1319]

$$\boldsymbol{\nabla} \times \boldsymbol{H} = \frac{\partial \boldsymbol{D}}{\partial t} + \boldsymbol{J}, \qquad (2.5)$$

$$\boldsymbol{\nabla} \times \boldsymbol{E} = -\frac{\partial \boldsymbol{B}}{\partial t}, \qquad (2.6)$$

$$\boldsymbol{\nabla} \cdot \boldsymbol{B} = 0, \qquad (2.7)$$

$$\boldsymbol{\nabla} \cdot \boldsymbol{D} = \rho. \qquad (2.8)$$

In **time-harmonic** case vectors are expressed with phasors. For example, we can write a time-harmonic electric field as [15 p. 338]

$$\boldsymbol{E}(x, y, z, t) = Re\{\boldsymbol{E}(x, y, z) e^{j\omega t}\}, \qquad (2.9)$$

where ω is angular frequency (rad/s), and $\boldsymbol{E}(x, y, z)$ is a vector phasor that contains information on direction, magnitude, and phase [15 p. 338]. Now **time-harmonic** Maxwell's equations can be written as [15 p. 339]

$$\boldsymbol{\nabla} \times \boldsymbol{E} = -j\omega \boldsymbol{B}, \tag{2.10}$$
$$\boldsymbol{\nabla} \times \boldsymbol{H} = \boldsymbol{J} + j\omega \boldsymbol{D}, \tag{2.11}$$
$$\boldsymbol{\nabla} \cdot \boldsymbol{D} = \rho, \tag{2.12}$$
$$\boldsymbol{\nabla} \cdot \boldsymbol{H} = 0. \tag{2.13}$$

Electromagnetic theory consists of Maxwell's equations and the constitutive laws, which are relations between the field intensities and flux densities. In isotropic (uniform in all orientations), non-dispersive (phase velocity of a wave does not depend on its frequency), linear media (characteristics of the medium does not depend on the strength of electric and magnetic fields) the constitutive equations are

$$\boldsymbol{D} = \varepsilon \boldsymbol{E}, \tag{2.14}$$
$$\boldsymbol{B} = \mu \boldsymbol{H}, \tag{2.15}$$
$$\boldsymbol{J} = \sigma \boldsymbol{E}, \tag{2.16}$$

where ε is the scalar permittivity (F/m), μ is the scalar permeability (H/m), and σ is the conductivity (S/m) of the media. In a lossy material the vector fields relating permittivity and permeability are complex numbers, and in non-isotropic media they are tensors (different values depending on the orientation).

2.2. The wave equation

The propagation of electromagnetic wave is described by Maxwell's equations. In determining the wave equation, the propagation of electromagnetic wave is assumed to be in a linear, homogeneous, isotropic and lossless material, with vacuum as special case [15 p. 340]. By assuming a time-varying electric field ($\frac{\partial \boldsymbol{E}}{\partial t} \neq 0$) in a lossless medium, from differential equations (2.5)-(2.8) and equations (2.14)-(2.16), we can derive the wave equation [15 p. 335]

$$\nabla^2 \boldsymbol{E} - \varepsilon\mu \frac{\partial^2 \boldsymbol{E}}{\partial t^2} = 0. \tag{2.17}$$

This is a criterion that the electric field should fulfill in order to have a propagating wave in media. Likewise, if magnetic field is assumed to be time-varying ($\frac{\partial \boldsymbol{H}}{\partial t} \neq 0$), the wave equation for magnetic field can be derived as [15 p. 335]

$$\nabla^2 \boldsymbol{H} - \varepsilon\mu \frac{\partial^2 \boldsymbol{H}}{\partial t^2} = 0. \tag{2.18}$$

Equations (2.17) and (2.18) represent vector wave equations in Cartesian coordinate system.

In **time-harmonic** case, the wave equations can be derived using the phasor forms of Maxwell's equations. In a linear, homogeneous, isotropic, lossless and source-free medium, characterized by $\rho = 0, \sigma = 0$, and $\boldsymbol{J} = 0$, the second order partial differential wave equations are [15 p. 340]

$$\nabla^2 \boldsymbol{E} + k^2 \boldsymbol{E} = 0, \tag{2.19}$$
$$\nabla^2 \boldsymbol{H} + k^2 \boldsymbol{H} = 0, \tag{2.20}$$

where k is the wave number (rad/m), which is expressed as $k = \omega\sqrt{\mu\varepsilon} = \frac{\omega}{u} = \frac{2\pi f}{u}$ (u is the velocity of electromagnetic wave in media (m/s) and ω is angular frequency (rad/s)). Equations (2.19) and (2.20) are homogeneous Helmholtz's equations, whose solutions should be determined using various boundary conditions.

2.2.1. Plane waves in lossless medium

A uniform plane wave is a special solution of Maxwell's equations, where the electric field **E** is assumed to have the same direction, same amplitude, and same phase in infinite planes perpendicular to the direction of propagation (similarly for **H**). In a plane wave, also the electric field **E** and magnetic field **H** are perpendicular to each other [15 p. 354]. In order to determine the plane wave equations, we use the homogeneous vector Helmholtz's equations (2.19) and (2.20).

The free space Helmholtz's equation (2.19) becomes

$$\nabla^2 \boldsymbol{E} + {k_0}^2 \boldsymbol{E} = 0, \tag{2.21}$$

where k_0 ($k_0 = \frac{\omega}{c} = \omega\sqrt{\mu_0\varepsilon_0}$) is the free space wave number (rad/m). In Cartesian coordinate system, equation (2.21) is equivalent to three scalar Helmholtz's equations, one each in the components E_x, E_y, and E_z. Thus, equation of a plane wave propagating in z-direction is derived from Helmholtz's scalar equation for the component E_x, and it is [15 p. 355]

$$E_x(z) = E_x^+(z) + E_x^-(z) = E_0^+ e^{-jk_0 z} + E_0^- e^{jk_0 z}, \tag{2.22}$$

where E_0^+ and E_0^- are arbitrary (and, in general, complex) constants that must be determined by boundary conditions. Figure 2.1 illustrates a plane wave propagating in the z-direction.

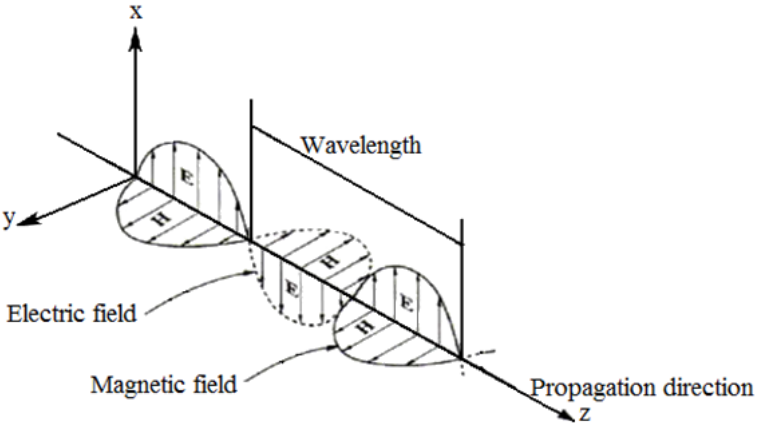

Figure 2.1. A plane wave propagating in the z-direction.

The propagation velocity of an equiphase front (the phase velocity) of a plane wave propagating in the z-direction in free space is equal to the velocity of light, which is determined with the equation

$$u_p = \frac{dz}{dt} = \frac{\omega}{k_0} = \frac{1}{\sqrt{\mu_0 \varepsilon_0}} = c \cong 3 \times 10^8 \,\mathrm{m/s}. \tag{2.23}$$

The magnetic field, **H**, of a plane wave is perpendicular to both the electric field and to the direction of propagation. Consequently, for a plane wave propagating in z-direction and having an electric field of $E_x(z)$, the magnetic field is [15 p. 357]

$$H_y(z) = \frac{k_0}{\omega \mu_0} E_x(z) = \frac{1}{\eta_0} E_x(z), \tag{2.24}$$

where η_0 is intrinsic wave impedance of free space, and it can also be written as

$$\eta_0 = \sqrt{\frac{\mu_0}{\varepsilon_0}} \cong 377\Omega. \tag{2.25}$$

Because η_0 is a real number, $H_y(z)$ is in phase with $E_x(z)$. Thus, for a uniform plane wave the ratio of the amplitudes of electric and magnetic field is equal to the intrinsic impedance of the medium [15 p. 357].

Polarization of plane waves

Polarization of a uniform plane wave describes the time-varying behavior of the electric field vector at a given point in space. For the case of a plane wave propagating in z-direction, electric field may only have components in the x- or y-directions. So in this case, the general expression for the electric field is [16 p. 119]

$$\boldsymbol{E}(z) = \left(E_{0x}\hat{\mathbf{x}} + E_{0y}\hat{\mathbf{y}}\right)e^{-jkz}, \tag{2.26}$$

where E_{0x} and E_{0y} are independent amplitudes of the x and y components. The polarization of the electromagnetic wave depends on the amplitude and phase of E_{0x} and E_{0y}. If $E_{0x} = 1$ and $E_{0y} = 0$, the field is linearly polarized in the x-direction. For example, equation (2.22) is the wave equation of a linearly polarized wave, because the electric field has just the E_x component. On the other hand, if $E_{0x} = E_{0y} = 1$, the field is linearly polarized in the direction of 45° between the x- and y-axes. In general, as long as E_{0x} and E_{0y} have the same phase, the wave will be linearly polarized [16 p. 119]

Electromagnetic wave can also be circularly polarized. In this case, the amplitudes of E_{0x} and E_{0y} are the same, but they have 90° phase difference. For instance, if $E_{0x}= 1$ and $E_{0y} = j$, electric field still lies in the x-y plane, but now rotates counterclockwise when viewed toward the z-axis. This can be seen by converting the phasor expression of (2.26) to the time domain by multiplying it with $e^{j\omega t}$ and taking the real part [16 p. 119]:

$$\begin{aligned}\boldsymbol{E}(z,t) &= Re\left\{(\hat{\mathbf{x}} + j\hat{\mathbf{y}})e^{-jkz}e^{j\omega t}\right\} \\ &= Re\left\{\hat{\mathbf{x}}e^{j(\omega t - kz)} + \hat{\mathbf{y}}e^{j(\omega t - kz + \frac{\pi}{2})}\right\} \\ &= \hat{\mathbf{x}}\cos(\omega t + kz) - \hat{\mathbf{y}}\sin(\omega t - kz).\end{aligned} \tag{2.27}$$

The equation (2.27) shows that for a given point on the z-axis, the electric field vector rotates from the x-axis to the –y-axis as time increases. Thus, the direction of rotation is counterclockwise when viewed toward the direction of propagation. This polarization is called left-hand circular polarization. Figure 2.2 illustrates the rotation of **E** as a function of time t, at $z = 0$ [16 p. 119].

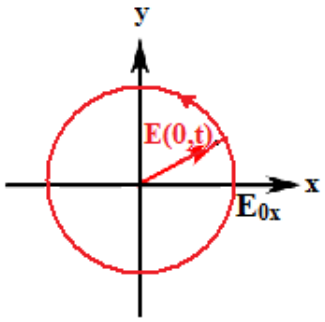

Figure 2.2. Circular polarization at $z = 0$.

Right-hand circular polarization can be obtained by changing the sign of the E_{0y} term. If the magnitudes of E_{0x} and E_{0y} are not the same, and the phase difference is not exactly 90°, then the most general case, the elliptical polarization, will be obtained [16 p. 119].

2.2.2. Plane waves in a lossy medium

So far, we have considered the propagation of electromagnetic waves in simple media without losses or dispersion. In lossless simple media, the permittivity and permeability of media is assumed constant scalar parameters in constitutive laws. But in general constitutive laws are not that simple. For instance, in a lossy simple (linear, homogeneous, and isotropic) media, losses cause a phase delay between the electric flux **D** and electric field **E**. In other words, in lossy simple media the permittivity is a complex number [14 p. 1287]. Consequently, in a lossy source-free medium the homogeneous vector Helmholtz's equation to be solved is [15 p. 367]

$$\nabla^2 \boldsymbol{E} + {k_c}^2 \boldsymbol{E} = 0, \tag{2.28}$$

where the wave number, k_c ($k_c = \omega\sqrt{\mu\varepsilon_c}$), is a complex number. Thus the wave number is a function of complex permittivity which is defined as [15 pp. 341-342]

$$\varepsilon_c = \varepsilon - j\frac{\sigma}{\omega} = \varepsilon' - j\varepsilon'', \tag{2.29}$$

where σ is conductivity (S/m), ε' is the real part of permittivity (F/m), and ε'' is the imaginary part of permittivity (F/m).

However, equation (2.28) can be presented using a propagation constant, γ, which is defined as [15 p. 367]

$$\gamma = jk_c = j\omega\sqrt{\mu\varepsilon_c} \ \ (\mathrm{m}^{-1}). \tag{2.30}$$

Since γ is a complex number

$$\gamma = \alpha + j\beta = j\omega\sqrt{\varepsilon\mu}\left(1 + \frac{\sigma}{j\omega\varepsilon}\right)^{\frac{1}{2}} = j\omega\sqrt{\varepsilon'\mu}\left(1 - j\frac{\varepsilon''}{\varepsilon'}\right)^{\frac{1}{2}}, \tag{2.31}$$

where α and β are the real and imaginary parts of γ, respectively. For a lossless medium, $\sigma = 0$ ($\varepsilon'' = 0, \varepsilon = \varepsilon'$), $\alpha = 0$, and $\beta = k = \omega\sqrt{\mu\varepsilon}$ [15 p. 367].
Using propagation constant, γ, the Helmholtz' equation becomes [15 p. 368]

$$\nabla^2 \boldsymbol{E} - \gamma^2 \boldsymbol{E} = 0. \tag{2.32}$$

Solution of the equation (2.32), representing a uniform plane wave propagating in the +z-direction, and assuming that the wave is linearly polarized in the x-direction, becomes [15 p. 368]

$$\boldsymbol{E} = \hat{\mathbf{x}}E_x = \hat{\mathbf{x}}E_0 e^{-\gamma z}. \tag{2.33}$$

The propagation factor $e^{-\gamma z}$ can be written as a product of two factors as

$$E_x = E_0 e^{-\alpha z} e^{-j\beta z}. \tag{2.34}$$

Both α and β in (2.34) are positive quantities. The first factor, $e^{-\alpha z}$, decreases as z increases, so α is an attenuation factor, and its SI unit is neper per meter (Np/m). The second factor, $e^{-j\beta z}$, is a phase factor. Thus, β is called a phase constant, and its SI unit is radians per meter (rad/m). The phase constant, β, expresses the amount of phase shift that occurs as the wave travels one meter [15 p. 368].

Good conductors

A good conductor has a high conductivity, so for a good conductor $\frac{\sigma}{\omega\varepsilon} \gg 1$. Consequently, it is convenient to use equation (2.31) and neglect 1 in comparison with the term $\frac{\sigma}{\omega\varepsilon}$. Doing this simplification for good conductors, the equation (2.31) becomes [15 p. 369]

$$\gamma \cong j\omega\sqrt{\mu\varepsilon}\sqrt{\frac{\sigma}{j\omega\varepsilon}} = \sqrt{j}\sqrt{\omega\mu\sigma} = \frac{1+j}{\sqrt{2}}\sqrt{\omega\mu\sigma} = (1+j)\sqrt{\pi f\mu\sigma}. \tag{2.35}$$

Equation (2.35) indicates that for good conductor factors α and β are approximately equal, and both increase as $\sqrt{f}$ and $\sqrt{\sigma}$ increase. Thus, for a good conductor [15 p. 369]

$$\alpha = \beta = \sqrt{\pi f\mu\sigma}. \tag{2.36}$$

Therefore, the phase velocity, u_p, and the wave length, λ, of a plane wave in a good conductor are [15 pp. 369-370]

$$u_p = \frac{\omega}{\beta} \cong \sqrt{\frac{2\omega}{\mu\sigma}} \text{ (m/s)}, \quad \lambda = \frac{2\pi}{\beta} = \frac{u_p}{f} = 2\sqrt{\frac{\pi}{f\mu\sigma}} \text{ (m)} \tag{2.37}$$

For instance, the phase velocity of copper is 720 m/s, which is about twice the velocity of sound in air and is many times slower than the velocity of light in air. The wave length of electromagnetic wave in copper, at 3 MHz, is 0.24 mm, while the wavelength of electromagnetic wave in air at this frequency is 100 m [15 p. 370]. So, in a good conductor, like copper, electromagnetic wave transforms to an AC electric current.

Since the attenuation factor is $e^{-\alpha z}$, the amplitude of the wave will be attenuated by a factor of e^{-1} when it travels a distance $\delta = \frac{1}{\alpha}$. On the other hand, the attenuation fac-

tor α is proportional to the square root of the conductivity σ and frequency f. Thus, electromagnetic wave attenuates very rapidly in a good conductor at high frequencies. The distance δ through which the amplitude of electromagnetic wave attenuates by a factor of e^{-1} or 0.368 is called skin depth. So, skin depth is [15 p. 370]

$$\delta = \frac{1}{\alpha} = \frac{1}{\sqrt{\pi f \mu \sigma}} \quad \text{(m)}. \tag{2.38}$$

Since in a good conductor $\alpha = \beta$, skin depth δ can also be written as

$$\delta = \frac{1}{\beta} = \frac{\lambda}{\sqrt{2\pi}} \quad \text{(m)}. \tag{2.39}$$

At microwave frequencies the skin depth of conductors is so small that fields and currents can be considered as confined in a very thin layer (that is, in the skin) of the conductor surface [15 p. 370].

The intrinsic impedance of a good conductor is [15 p. 369]

$$\eta_c = \sqrt{\frac{\mu}{\varepsilon_c}} \cong \sqrt{\frac{j\omega\mu}{\sigma}} = (1+j)\sqrt{\frac{\pi f \mu}{\sigma}} = (1+j)\frac{\alpha}{\sigma} \quad (\Omega), \tag{2.40}$$

which has a phase angle of 45°. So in a conductor the magnetic field intensity lags behind the electric field intensity 45°.

2.3. Boundary conditions

Electromagnetic problems usually deal with situations, where electrical properties of medium change rapidly. Thus, it is necessary to know the behavior of electric- and magnetic fields at the interface of two medium. In other words, there are boundary conditions that field vectors **E**, **D**, **H**, and **B** must satisfy at the interfaces. The boundary conditions are derived by applying the integral form of Maxwell's equations to a small region at an interface of two mediums, because the integral equations are assumed to hold for regions containing discontinuous media [15 p. 329].

The boundary conditions for the vector fields **E** and **H** are [13 p. 23]

$$\boldsymbol{n} \times (\boldsymbol{E}_1 - \boldsymbol{E}_2) = \boldsymbol{0}, \tag{2.41}$$

$$\boldsymbol{n} \times (\boldsymbol{H}_1 - \boldsymbol{H}_2) = \boldsymbol{J}. \tag{2.42}$$

According to the equation (2.41) the tangential component of **E** field is continuous across an interface. The boundary conditions for the normal components of **B** and **D** are defined as [13 p. 23]

$$\boldsymbol{n} \cdot (\boldsymbol{D}_1 - \boldsymbol{D}_2) = \rho, \tag{2.43}$$
$$\boldsymbol{n} \cdot (\boldsymbol{B}_1 - \boldsymbol{B}_2) = 0. \tag{2.44}$$

Equation (2.43) states that the normal component of **D** field is discontinuous across an interface where a surface charge exists, and the amount of discontinuity is equal to the surface charge density ρ. But according to the equation (2.44) the normal component of **B** field is continuous across an interface.

At the interface of a lossless medium and a good conductor ($\sigma = \infty$), fields in the lossless medium fulfill the boundary conditions presented above. Although, there exist no material with infinite conductivity, but in electromagnetic modeling of ‘‘good conductors’’ such as copper, silver, gold, and aluminum, we can use the presented interface conditions. But at the interface of two lossless medium there exist no surface current ***J*** and surface charge density ρ. So in this case, also **H** and **D** fields are continuous across the interface [13 p. 24].

Usually electromagnetic problems are modeled with partial differential equations, such as Helmholtz equation. Without boundary conditions, partial differential equations have infinite number of solutions. So boundary conditions are needed to find a unique solution for a partial differential equation.

2.4. Electromagnetic energy and power

Electromagnetic waves carry with them electromagnetic power, and transport energy through space over long distances. Let’s consider a closed surface S which includes a volume V with relative permittivity ε_r, relative permeability μ_r and conductivity σ. Electromagnetic energy source **J** in the space V cause electromagnetic fields. Complex power delivered by the sources is given as [13 p. 31]

$$P_s = -\frac{1}{2}\int_V (\boldsymbol{E} \cdot \boldsymbol{J}^*) dV. \tag{2.45}$$

The time-average stored electric energy in a volume V is [13 p. 32]

$$W_e = \frac{1}{4} Re \int_V \boldsymbol{E} \cdot \boldsymbol{D}^* dV = \frac{\varepsilon_0}{4}\int_V \varepsilon_r' |\boldsymbol{E}|^2 dV. \tag{2.46}$$

Similarly, the time-average magnetic energy stored in the volume V is [13 p. 32]

$$W_m = \frac{1}{4} Re \int_V \boldsymbol{H} \cdot \boldsymbol{B}^* dV = \frac{\mu_0}{4}\int_V \mu_r' |\boldsymbol{H}|^2 dV. \tag{2.47}$$

The complex power flow out of the closed surface S of the volume V is defined as Poynting vector **S** (W/m^2), as [13 p. 32]

$$\boldsymbol{S} = \boldsymbol{E} \times \boldsymbol{H}^*, \tag{2.48}$$

and the time-average power leaving the boundary of the volume V can be expressed as [13 p. 32]

$$P_0 = \frac{1}{2} Re \int_{\partial V} \boldsymbol{E} \times \boldsymbol{H}^* \cdot \boldsymbol{dS}. \tag{2.49}$$

The time-average power dissipated in the volume V due to conductivity, dielectric, and magnetic losses can be defined as [13 p. 32]

$$P_l = \frac{1}{2} \int_V \sigma |\boldsymbol{E}|^2 \, dV + \frac{\omega}{2} \int_V (\varepsilon_0 \varepsilon_r'' |\boldsymbol{E}|^2 + \mu_0 \mu_r'' |\boldsymbol{H}|^2) dV. \tag{2.50}$$

Then, with the above definitions, the power balance equation in frequency domain (Poynting's theorem) can be rewritten as [13 p. 32]

$$P_s = P_0 + P_l + 2j\omega(W_m - W_e). \tag{2.51}$$

The complex power balance equation (2.51) states that the power delivered by the sources (P_s) is equal to the sum of the power transmitted through the surface (P_0), and the power lost to heat in the volume (P_l), and 2ω times the net reactive energy stored in the volume [13 p. 32].

3. BASICS OF ANTENNA THEORY

Antennas are electrically conducting structures, which can be used in both transmitting and receiving electromagnetic waves. In transmission, an oscillating current in the antenna excites electromagnetic waves in distinct directions. On the other hand, in reception, when the antenna receives an electromagnetic wave from space, the charge carriers start moving in the antenna resulting in an electric current. In other words, antenna is the transitional structure between the free-space and a transmission line device. The art of antenna design is to ensure that conversion of energy between two modes of oscillating current and electromagnetic wave takes place as efficiently as possible.

3.1. Types of antennas

In this section some forms of various antenna types are introduced and discussed briefly.

3.1.1. Wire antennas

Wire antennas are seen everywhere; on buildings, ships, automobiles, and so on. There are many types of wire antennas, such as dipole, loop, and helix. A dipole antenna is a linearly polarized antenna, whose length is proportional to the wavelength of the electromagnetic wave. Loop antenna can take the form of a rectangle, square, ellipse, or any other configuration. The circular loop is the most common because of its simplicity in construction.

3.1.2. Aperture antennas

Aperture antennas are mostly used at microwave and millimetre-wave frequencies [14 p. 365]. The geometry of the aperture antenna can be circular, square, rectangular, elliptical, or any other shape. Figure 3.1 shows a few structures of aperture antennas.

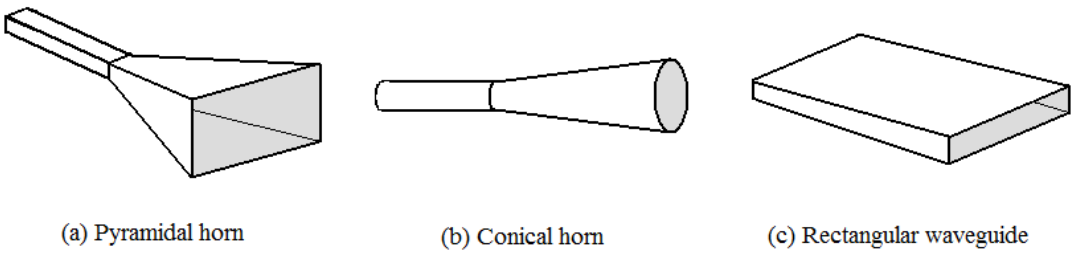

Figure 3.1. Aperture antenna configurations.

Aperture antennas are widely used in aerospace applications, because they can be flush-mounted onto the spacecraft or aircraft surface. The aperture opening can be covered with a dielectric material that is transparent to the RF energy to protect the antenna from environmental conditions.

3.1.3. Microstrip antennas

Microstrip antennas consist of a metallic patch on a grounded substrate. The patch can take many different configurations. Rectangular and circular patches are very common, because of ease of analysis and fabrications. Microstrip antennas are used widely, because they are inexpensive, suitable to planar and non-planar surfaces, simple, and inexpensive to fabricate using modern printed-circuit technology. Additionally, they are very robust when mounted on rigid surfaces and they are very versatile in terms of the resonance frequency, polarization, pattern, and impedance [17 p. 5].

Microstrip antennas can be mounted on surface of aircraft, spacecraft, satellite, missiles, mobile phones, and so on.

3.1.4. Antenna arrays

Antenna array consists of two or more antenna elements arranged linearly (along a line), two dimensionally (arranged in a plane), or three dimensionally. Antenna arrays are used in applications which require radiation characteristics that may not be achievable by a single element antenna. The group of antenna can be arranged such that the oscillating electric and magnetic fields of the radiating elements add up in specific directions resulting in a maximum, and cancel in some desired directions resulting in a minimum [17 p. 6].

3.1.5. Reflector antennas

Reflector antennas reflect the incoming electromagnetic wave emitted by a feed antenna, when the feed antenna is placed at the focal point of the reflector antenna. There are different reflector types such as plane reflector, parabolic reflector and corner reflector. Reflector antennas are used in transmitting or receiving signals that travel millions of kilometres. Antennas of this type have been built with diameters as large as 305m. Such large dimensions are needed to achieve the high gain required to transmit or receive signal over millions of kilometres. Reflector antennas are used especially in satellite applications (satellite dish antenna), and in the exploration of outer space [17 p. 6].

3.2. Radiation mechanism

According to Maxwell's equations, radiation occur when the charges accelerate or decelerate in a wave guide structure [18 p. 62]. Figure 3.2 shows a circular cylinder of

cross-sectional area of A and volume V, where is distributed an electric volume charge density, represented by q_v (C/m3).

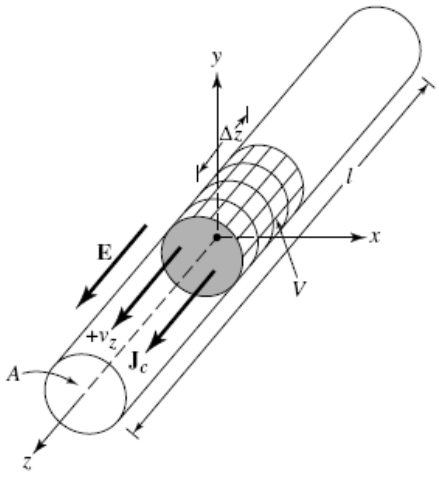

Figure 3.2. A conductive cylinder of cross-sectional area of A and volume V [17 p. 9].

The total charge Q is moving in the z-direction with a uniform velocity v_z (m/s). The current density J_z over the cross section of the wire is given by [17 p. 9]

$$J_z = q_z v_z. \tag{3.1}$$

If the wire is made of perfect electric conductor, the surface current density, J_s (A/m), resides on the surface of the wire, and it is given by

$$J_s = q_s v_z, \tag{3.2}$$

where q_s is the surface charge density (C/m^2). On the other hand, if the wire is very thin (ideally zero radius), then the current in the wire can be represented by

$$I_z = q_l v_z, \tag{3.3}$$

where q_l is the charge per unit length (C/m). For further investigation, it is sufficient to concentrate on the very thin wire case, because the conclusions apply to all three. For a time varying current, equation (3.3) can be written as

$$\frac{dI_z}{dt} = q_l \frac{dv_z}{dt} = q_l a_z, \tag{3.4}$$

where a_z is the acceleration (m/s^2). If the wire is of length l, then equation (3.4) can be written as

$$l\frac{dI_z}{dt} = lq_l\frac{dv_z}{dt} = lq_l a_z. \tag{3.5}$$

Equation (3.5) is the basic relation between current and charge, and it also serves as fundamental relation of electromagnetic radiation [19], [20]. Equation (3.5) states that to create radiation, there must be a time-varying current or an acceleration (or deceleration) of charge. For instance, in the case of Figure 3.3 (a), a group of charges in uniform motion (or stationary charges) in a straight and infinitely long wire do not produce radiation. But radiation occurs if the wire is curved, bent, discontinuous, terminated, or truncated, as shown in Figure 3.3 (b)-(f).

When the wire is curved or bent the speed of the charges remain constant, but their direction is changing, thereby creating radiation [18]. In the case of a discontinuous wire, the speed of the charges change causing charge acceleration and creating radiation. In Figure 3.3 (e), the wire is initially energized and the charges are accelerated in the source end of the wire and decelerated during reflection from its end. Thus, radiation is created at each end and along the remaining part of the wire [21]. In the case of Figure 3.3 (f), charges reach the end of the wire and reveres direction producing radiation [18]. In all these cases, radiation is caused by charge acceleration (or deceleration) [19][21]. Radiation happens also in the case of an oscillating charge in time-motion.

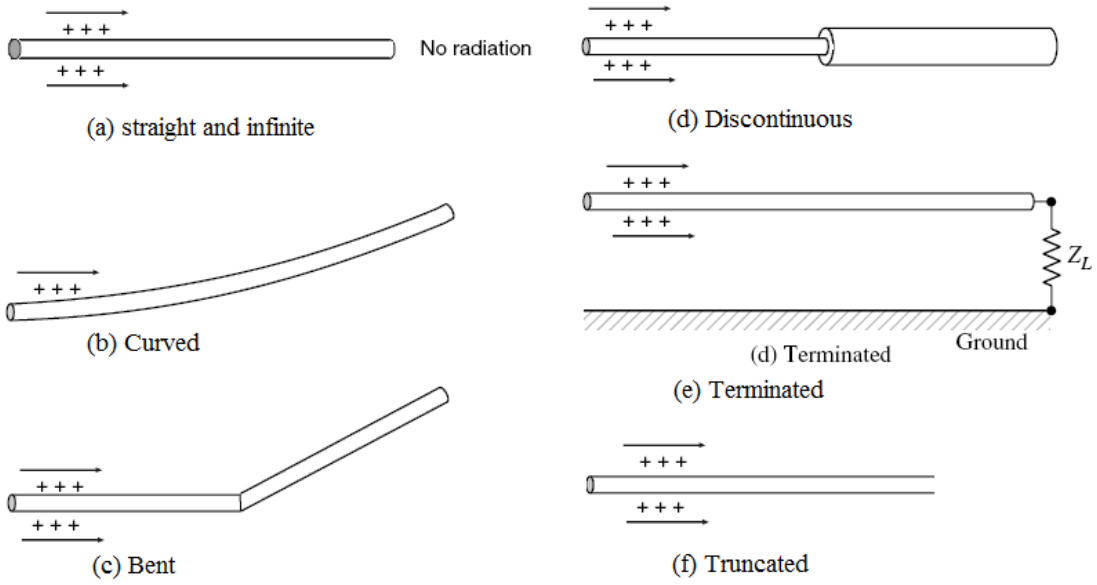

Figure 3.3. Wire configurations for radiation.

Antennas can therefore be seen as devices which cause charges to be accelerated in ways which produce radiation with desired characteristics. Although, both current density, $\boldsymbol{J}_c$, and charge density, q_v, appear as source terms in Maxwell's equations, charge is viewed as a more fundamental quantity, especially for transient fields [19].

3.3. Antenna parameters

Antennas are reciprocal. This means that their transmission and reception characteristics are the same. Because of this reciprocity it is sufficient to analyze antenna properties either in transmission mode or in reception mode. These properties are described by certain antenna parameters, depending on the application. Definitions of the most essential antenna parameters will be given in this chapter.

3.3.1. Field regions

The surrounding space of antenna is usually divided into three regions; reactive near field, radiating near field, and far field regions. Although there are no abrupt changes when crossing the boundary of these regions, there are significant differences in the field at different regions. The boundaries separating these regions are not unique, but there are various criteria that have been established, and are commonly used to identify these regions [17 p. 34][22].

The definition of the boundaries varies depending on the application and the amount of error an application can tolerate. For instance, the boundaries can be determined through an algebraic approach, using the field definitions of the elemental electric dipole and the elemental magnetic loop antenna. Another approach is defining the boundary by considering the change of wave impedance in the function of distance from a source. Shield designers use this approach. Antenna designers usually examine the boundary location by considering the effect of distance from an antenna to the phase of launched waves[22]. This section will present the common definitions of boundaries from an antenna designer's point of view. Figure 3.4 illustrates the field regions.

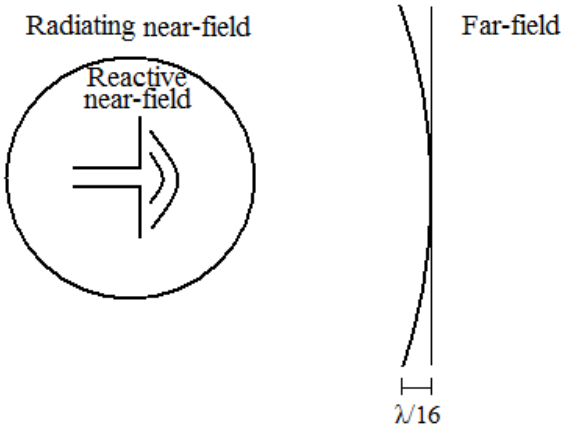

Figure 3.4. Field regions of an antenna.

Reactive near field is the surrounding region nearest to the antenna. At this region reactive field dominates over the radiative fields. For most antennas, the outer boundary

of this region exists at a distance $0.62\sqrt{D^3/\lambda}$ (as long as D >> λ) from the antenna surface, where D is the largest dimension of the antenna and λ is the wavelength [17 p. 34].

Radiating near field (Fresnel) region locates between the reactive near field region and far field region. At this region radiation fields predominate, and the angular field distribution is dependent upon the distance from the antenna [17 p. 34]. If the antenna's maximum dimension is not large compared to the wavelength, this region may not exist. For an antenna focused at infinity, the radiating near field is sometimes referred to as the Fresnel region on the basis of analogy to optical terminology. The inner boundary of this region is taken to be the distance $R > 0.62\sqrt{D^3/\lambda}$ and the outer boundary the distance $R < 2D^2/\lambda$, when D is the maximum dimension of the antenna [17 p. 34].

Far-field (Fraunhofer) region is the region where the angular field distribution is essentially independent of the distance from the antenna [17 p. 35]. At this region the spherical wave front radiated by an antenna becomes a close approximation to the ideal planar phase front of a plane wave.

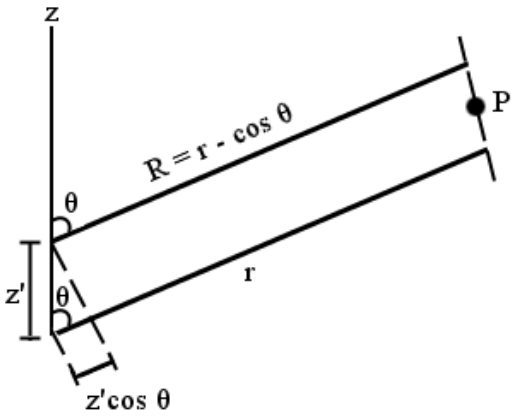

Figure 3.5. Parallel ray approximation for far-field calculations of a line source.

Figure 3.5 shows a situation where a line source is placed along the z-axis, and the observation point is far (ideally, at the infinite distance) from the line source. If parallel lines (or rays) are drawn from each point from a line current, the distance *R* to the observation point is related to *r* by

$$R = r - z' \cos\theta, \tag{3.6}$$

where z' is the distance between two parallel rays, *r* is the distance of the observation point from the origin, and *R* is the distance of another array to the observation point.

The parallel ray equation is exact only when the observation point is at infinity, but it is a good approximation at the far field. In practice, the far field begins at a distance *r*, where the error due to the approximation is a sixteenth of a wavelength. This corresponds to a phase error of $2\pi/\lambda \cdot \lambda/16 = \pi/8 = 22.5°$ [23 pp. 29-31]. At the far field

region, the actual spherical wave front radiated from the antenna differs less than 22.5° from a true plane wave front over the maximum extent of the antenna [16 p. 114]. Considering exact relation of the distance R and r, and the phase error 22.5°, the far field condition can be derived as the distance $r > 2D^2/\lambda$ [16 p. 114], [23 pp. 29-31].

3.3.2. Radiation pattern

No antenna can radiate isotropically. In other words, no antenna can radiate in all directions equally. So a radiation pattern is always needed to determine the antenna parameters [13 p. 157]. Radiation pattern is a three-dimensional graph of radiated power of antenna versus angles ϕ (azimuth) and θ (elevation) in a polar coordinate system, when the antenna is placed at the origin. Figure 3.6 shows the polar coordinate system.

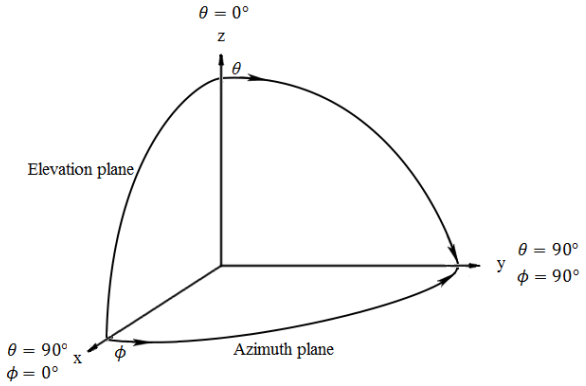

Figure 3.6. Polar coordinate system.

Usually the radiation pattern is represented by principal plane wave pattern plots, such as **E**-plane and **H**-plane. For instance, in the **E**-plane plot of a dipole placed at the origin along the z-axis, the angle ϕ is held fixed while θ is varied, and likewise in the **H**-plane plot the angle θ is held fixed while angle is varied [15 p. 608]. Figure 3.7 shows the **E**-plane (elevation plane) and the **H**-plane plots of a dipole (l=0.1λ) placed at the origin along the z-axis.

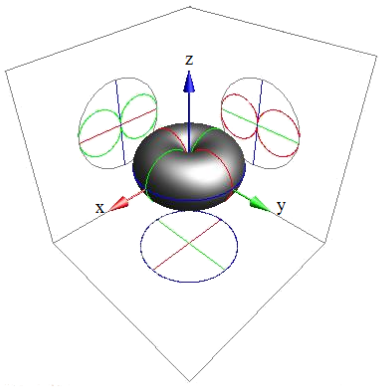

Figure 3.7. Radiation pattern of a center-fed linear dipole antenna with a sinusoidal current distribution [24].

From a radiation pattern we can recognize distinct radiation lobes, with different maxima in different directions. The radiation lobe having the maximum value is called the main beam, while those lobes at lower levels are called sidelobes.

Another fundamental parameter that can be seen from a radiation pattern is the 3dB angular beam width of the antenna. An antenna with a broad main beam can transmit/receive signal over a wide angular region, while an antenna having narrow main beam can transmit/receive power over a small angular region. The 3 dB beam width is defined where the power density of the radiated wave is dropped 3 dB in the main beam [16 p. 116].

3.3.3. Directivity

In addition to the beam width of an antenna, also directivity is a measure of the focusing ability of an antenna. Directivity is defined as the ratio of the maximum radiation intensity (W/rad^2) in the main beam to the average radiation intensity (W/rad^2) over all space [16 p. 116]. Stated more simply, the directivity of an antenna is equal to the ratio of its radiation intensity in a given direction over that of an isotropic source. The average radiation intensity is equal to the total power radiated by the antenna divided by 4π. Thus, mathematically directivity is defined as

$$D = \frac{U_{max}}{U_{avg}} = \frac{4\pi U_{max}}{P_r}, \tag{3.7}$$

where P_r is radiated power. Directivity is dimensionless, and is usually expressed in dBi (compared to the gain of isotropic antenna) [16 p. 116].

3.3.4. Input impedance

Input impedance is defined as the impedance presented by an antenna at its terminals. In other words, the ratio of the voltage to current at the terminals of an antenna defines the impedance of the antenna as

$$Z_A = R_A + jX_A, \tag{3.8}$$

where R_A is antenna resistance at terminals (Ω), and X_A is antenna reactance at terminals (Ω). The antenna resistance consists of two components; that is

$$R_A = R_r + R_L, \tag{3.9}$$

where R_r is the radiation resistance of the antenna, and R_L is the loss resistance of the antenna. The loss resistance, R_L, represents the conduction and dielectric losses. On the other hand, radiation resistance is a measure of the amount of power radiated by an an-

tenna. The radiation resistance of an antenna is the value of a hypothetical resistance that would dissipate the amount of power equal to the radiated power P_r when the current in the resistance is equal to the power supplied to the terminals of the antenna. Additionally, the radiation resistance depends on the geometry and the substrate of the antenna, not on the material of the radiating element of the antenna. Naturally a high radiation resistance is desirable for the antenna [15 p. 612].

At high frequencies the resistance caused by conduction losses of the antenna is different from the DC resistance [17 p. 86]. For example, for a metal rod of length l and uniform cross-sectional area A, the DC resistance is given by [17 p. 86]

$$R_{dc} = \frac{1}{\sigma}\frac{l}{A}, \tag{3.10}$$

where σ is the conductivity of the metal.

When frequency increases, the skin depth δ (2.38) is much smaller than the conductor radius, and current confines to a thin layer near the conductor surface [17 p. 86]. Hence, the high-frequency resistance, based on a uniform current distribution along the length of the rod, is given as [17 p. 86]

$$R_{hf} = \frac{l}{P}R_s = \frac{l}{P}\sqrt{\frac{\omega\mu_0}{2\sigma}}, \tag{3.11}$$

where P is the perimeter of the cross section of the rod ($P = 2\pi b$ for a circular wire of radius b), R_s is the conductor surface resistance (Ω), ω is the angular frequency (rad/s), μ_0 is the permeability of free-space (H/m), and σ is the conductivity of the metal (S/m).

3.3.5. Radiation efficiency

All antennas have conduction, and dielectric losses. Such losses result in a difference between the power delivered to the input of an antenna and the power radiated by that antenna [16 p. 117]. In other word, radiation efficiency can be defined as the ratio of the desired output power to the supplied input power

$$e = \frac{P_r}{P_{in}} = \frac{P_r}{P_r + P_L} = \frac{P_{in} - P_L}{P_{in}} = 1 - \frac{P_L}{P_{in}}, \tag{3.12}$$

where P_r is the power radiated by the antenna (W), P_{in} is the power supplied to the terminals of the antenna (W), and P_L is the power lost in the antenna (W) [16 p. 117].

Radiation efficiency can also be defined as the ratio of the power delivered to the radiation resistance R_r to the power delivered to the radiation resistance R_r and the loss resistance R_L. So, mathematically radiation efficiency is expressed as [17 p. 86]

$$e = \frac{R_r}{R_L + R_r}. \tag{3.13}$$

3.3.6. Gain

Directivity of an antenna is only a function of the radiation pattern of the antenna, and it does not account for the efficiency or the input impedance of the antenna. A practical antenna with radiation efficiency less than unity cannot radiate all of its input power. To account for this, antenna gain is defined as the product of directivity and efficiency. So the gain G of an antenna is [16 p. 118]

$$G = eD. \tag{3.14}$$

Equation (3.14) shows that gain is always equal to the directivity or less than it. The antenna gain can also be computed by replacing P_{rad}, in the dominator of equation (3.7) with P_{in}. So, the equation for gain is [16 p. 118]

$$G = eD = \frac{P_r}{P_{in}} \frac{4\pi U_{max}}{P_r} = \frac{4\pi U_{max}}{P_{in}}. \tag{3.15}$$

Gain is usually expressed in dBi (compared to the gain of isotropic antenna).

3.3.7. Quality factor and bandwidth

Quality factor, bandwidth and efficiency of an antenna are interrelated, and no one of these can be optimized separately. Therefore, there is always a tradeoff between them in arriving an optimum antenna performance. Quality factor is representative of the antenna losses (radiation, conduction, dielectric and surface wave losses), so the total quality factor is written as [17 p. 852]

$$\frac{1}{Q_t} = \frac{1}{Q_r} + \frac{1}{Q_c} + \frac{1}{Q_d} + \frac{1}{Q_{sw}}, \tag{3.16}$$

where
Q_t = total quality factor
Q_r = quality factor due to radiation losses
Q_c = quality factor due to conduction (ohmic) losses
Q_d = quality factor due to dielectric losses, and
Q_{sw} = quality factor due to surface waves.

For very thin substrates the surface wave losses are very small and can be neglected. However, for thicker substrates they need to be taken into account [25]. Equations for quality factors due to radiation, conduction, dielectric, and surface wave losses differ depending on the antenna configuration. For example, for a microstrip antenna which

has very thin substrate there are approximate formulas to represent the quality factors of conductivity, radiation, and dielectric losses. These approximate formulas are [17 p. 853]

$$Q_c = h\sqrt{\pi f \mu \sigma}, \tag{3.17}$$

$$Q_d = \frac{1}{\tan\delta}, \tag{3.18}$$

$$Q_r = \frac{2\omega\varepsilon_r}{h\, G_t/l} K, \tag{3.19}$$

where $\tan\delta$ is the loss tangent of the substrate material, σ is the conductivity of the conductors associated with the patch and ground plane, G_t/l is the total conductance per unit length of the radiating aperture, and K is [17 p. 853]

$$K = \frac{\iint_{area} |E|^2 dA}{\oint_{perimeter} |E|^2 dl}. \tag{3.20}$$

According to equation (3.19), Q_r is inversely proportional to the height of substrate, and for very thin substrates it is usually the dominant factor.

The fractional bandwidth of antenna is inversely proportional to the total quality factor Q_t of the antenna, and it is defined as [17 p. 853]

$$\frac{\Delta f}{f_0} = \frac{1}{Q_t}. \tag{3.21}$$

Equation (3.21) does not take into account impedance matching at the input terminals of the antenna. A better definition for the fractional bandwidth is over a band of frequencies where the VSWR (it measures the amount of voltage reflected back, in a transmission line, toward the source due to impedance mismatch; there are no reflections when VSWR is 1:1, and all the transmitting wave is reflected when VSWR is infinite) at the input terminals is equal to or less than a desired maximum value, assuming that the VSWR is unity at the design frequency. Equation for bandwidth that takes into account impedance matching is[17 p. 854]

$$\frac{\Delta f}{f_0} = \frac{VSWR - 1}{Q_t\sqrt{VSWR}}. \tag{3.22}$$

4. RADIO FREQUENCY IDENTIFICATION

Radio Frequency Identification (RFID) technology allows wireless identification of objects. The major components of RFID system are transponders known as tags that are attached to objects and contain information about the object, and interrogators known as readers that communicate wirelessly with the tags to enable identification. Both readers and tags need an antenna or antennas to communicate via it. RFID systems exist in various contexts that can be classified based on the frequency of operation, power source of the tag and the method of communication between the reader and the tag. A detailed classification of the commercial RFID systems based on the above criteria is presented in this chapter.

At the highest level, RFID systems can be divided into two classes based on the power source of the tags; active and passive. Active tags require a power source. They are either connected to a powered infrastructure or use a battery [26]. Batteries make the cost, size, and lifetime of active tags. Passive RFID tags do not require batteries and provide their energy from the radio wave transmitted to them by the reader antenna, and communicate with the reader by controlled reflection (backscattered wave) of a portion of this incident wave. Passive tags also have an indefinite operational life and are small enough to fit into a practical adhesive label [26]. In this chapter we focus on passive UHF RFID systems.

The goal of commercial RFID systems is to automate and enhance asset management. For instance, RFID systems can be used in applications such as supply chain management[27], indoor asset and personnel tracking[28], access control[29][30], and many more. The increasing use of RFID systems is due to the numerous advantages of the system over traditional identification mechanisms such as barcodes. Passive RFID tags can be read at much longer distances than barcodes. In addition, there is no need for a line of sight between the reader and the tag, and multiple tags can be read at much higher rates than barcodes. RFID tags have a large memory which allows storage of a lot more information than just the ID, and the information contained in the RFID tag can be modified dynamically using the reader [31].

4.1. Passive RFID system

As it is mentioned above RFID system consists of a reader, a tag, and antennas. Figure 4.1 shows a simplified structure of an RFID system. The antenna or antennas of the reader can be integrated with the reader, or it can be physically separate and connected with a cable. The reader is a two way radio transmitter-receiver that sends a signal to a tag and reads its response.The tag antenna is always physically integrated with the tag.

Most tags have at least one integrated circuit (IC), often known as a chip. The chip contains the tag ID and the logic needed to navigate the protocol that guides discussions between the tag and reader. The reader may have a user interface, or it can be connected to a host computer, which interacts with the user to control the reader. Additionally the computer stores and displays the resulted data from the tag chip [32 p. 22].

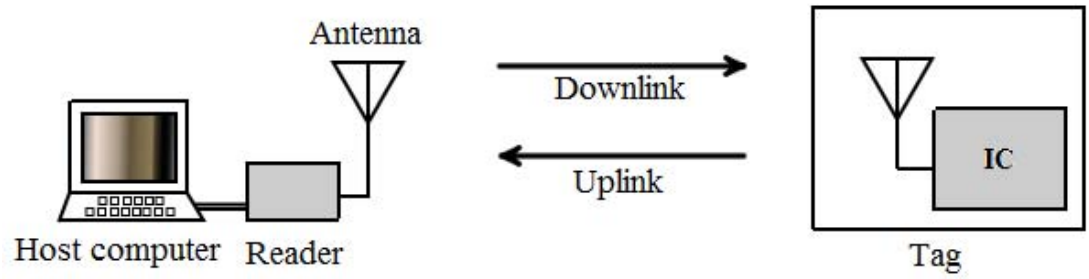

Figure 4.1. RFID system.

The radio link between the reader and the tag is a two way radio link. Although they use the same physical space and use the same antennas, they are distinguishable between the communication channel carrying information from the reader to the tag (the downlink or forward link), and that carrying information from the tag to the reader (uplink or reverse link) [32 p. 22]. An RFID reader transmits an encoded radio signal to the tag. The tag receives the message by its antenna, and the chip responds back by modulating the backscattering signal from the tag antenna, and so conveying the information stored in it to the reader antenna. This information may be only a unique tag serial number, or may be a product-related information such as a stock number, lot or batch number, production date, or other specific information [32 p. 22].

4.2. Frequency bands for RFID

RFID systems are classified based on the frequency region of the electromagnetic waves they use. The choice of frequency, power source, and protocol has important implication for range, cost, and features available. RFID systems use frequencies from around 100 kHz to over 5 GHz. The most commonly used frequency bands for RFIDs are the 125/134 kHz, 13.56 MHz, 860-960 MHz, and 2.4-2.45 GHz (Figure 4.2)[31][32 p. 24].

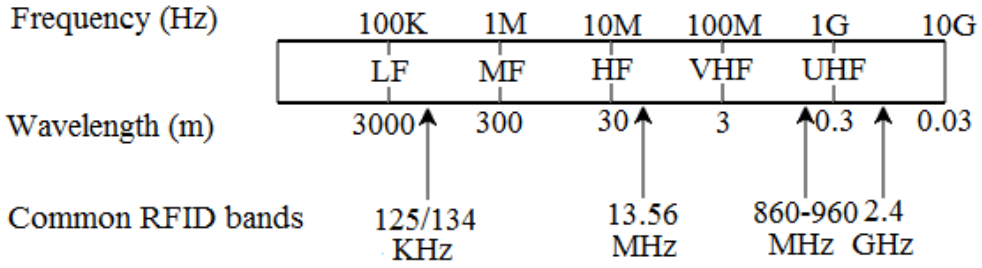

Figure 4.2. RFID frequency bands.

RFID systems working in 125/134 kHz frequency band work in low-frequency (LF) band, and are often referred to as LF tags and readers. Systems working in 13.56 MHz frequency band work in high-frequency (HF) band, and are referred to as HF tags and readers. RFID systems in 900 MHz region and 2.4 GHz region are both within the ultra-high-frequency (UHF) band, but in order to make a convenient distinction between these two, 900 MHz readers and tags are often referred to as UHF devices, whereas 2.4 GHz systems are known as microwave devices[32 pp. 24-30].

Wavelength differs significantly in the frequency regions RFID systems use. For instance the wavelength of a wave with 125 kHz is 2.4 km, while the wavelength in 900 MHz is 33 cm. Naturally RFID antennas in LF region are small compared to the wavelength. There are RFID systems with antennas comparable to wavelength in size, and RFID systems with antennas extremely smaller than a wavelength [32 pp. 24-30].

Systems where the wavelength is much larger than the antenna are typically inductively coupled. In this case, almost all the available energy from the reader antenna is contained in the near field region of the reader antenna. In this region the energy falls away as the cube of distance. Within this region, communication between the tag and the reader is effectively instantaneous, since the propagation time to the tag is a small fraction of time for a complete cycle of a RF voltage. In this case, it is difficult to distinguish the forward- and reverse link. The reader-tag system acts as a magnetic transformer providing coupling between the current flowing in the reader and the voltage across the tag. So in this case, we think of changes caused by the tag antenna as inducing changes in the electrical impedance of the reader antenna [32 pp. 24-30].

In RFID systems where the antenna is comparable to wavelength in size, communication happens through radiative coupling. In other words, in this case communication happens in the far field region of the reader antenna. The intensity of power radiated from the reader antenna falls off as the square of the distance travelled and the wave interacts with the tag antenna at some distinguishably later time much longer than an RF cycle. Then, a distinct scattered wave returns to the reader; the total round trip transit time is much longer than a RF cycle [32 pp. 24-30].

Here is a list of the most important features of RFID systems for different frequency regions [32 pp. 31-32]:

- LF- and HF RFID systems involve inductive coupling. LF- and HF tags use coil antennas, where the voltage induced is proportional to the number of turns of the coil, the size of the coil, and the frequency of the operation. LF tag coil antennas have many turns, while HF antennas need fewer.
- UHF RFID systems use generally radiative coupling. In radiative coupling the tag antennas are not coils but variants of planar antenna configurations. These tags have much longer read ranges than that of tag antennas using inductive-coupling, because UHF tag antennas communicate with the reader antenna in its far field region.
- Inductively coupled read zones are generally small and simple; radiative coupled read zones are larger but complex and often discontinuous, and nearby readers can interfere with each other.
- LF radiation penetrates water and common aqueous materials to a distance much longer than the read range of a typical system. HF penetration into water is comparable to read range of the system, and UHF/microwave penetration into water is negligible compared to typical read range in air.
- LF radiation can penetrate thin layers of conductive materials; HF and UHF radiation are effectively shielded by even quite thin films or metals.
- LF tags are limited to low data rates, whereas HF and UHF tags can supply tens or hundreds of kbps.

The differing characteristics of each frequency band mean that the suitable applications are different for each band. For instance LF tags and readers are appropriated for human and animal ID, HF tags are widely used for asset tracking and supply management, and UHF tags are used in automobile tolling and rail-car tracking, where ranges of several meters add considerable installation flexibility [32 p. 32].

4.3. RFID components

As it is mentioned in the section 4.1, RFID system consists of a two way radio transmitter-receiver, a reader, and a tag. The tag consists of the tag antenna and an IC which contains the information that should be read by the reader [32]. This section discusses the RFID components in more details.

4.3.1. RFID tag

There are three kinds of tags characterized by the power feeding method; passive tags, semi-passive tags, and active tags. It is often advantageous to eliminate the radio transmitter and battery from the tag to save money and space. On the other hand, the presence of radio transmitter and battery in the tag enables long read ranges and more facilities for the tag.

Active tags have battery, receiver, transmitter, and control circuitry, and are thus configured as bidirectional radio communication devices. The active tag synthesizes a

carrier signal using a local oscillator and a crystal reference, so it can communicate within a specific frequency band and it can also use different frequency channels in the presence of other tags. The read ranges of active tags are measured in hundreds of meters and even in kilometres, depending on the environment, transmit power, and frequency bands. This is due to significant transmitting power and filtering and amplification to provide good receive sensitivity [32 pp. 39-40].

Semi-passive tags, also known as battery-assisted passive tags, have a local battery to power the tag circuitry, but still use backscattered communications for the tag-to-reader (uplink) communications. Due to presence of battery, it is possible to add high-frequency amplification and other RF devices in the cost of increase in size, cost, and maintenance requirement. The read ranges of semi-passive tags are measured in tens of meters to as much as 100 m. Semi-passive tags are used in automobile tolling applications and in tracking of airplane parts and other reusable high-value assets [32 p. 38].

Passive tags have no independent source of electrical power to derive the circuitry in the tag, and they neither have a radio transmitter. Passive tags provide their power by rectifying the received signal from the reader antenna. When having enough power, the IC modifies the tag antenna's backscattering power corresponding with the information saved in the IC memory in order to send information back from the tag to the reader [32 p. 34].

A simplified structure of a passive tag is shown in Figure 4.3. When an electromagnetic wave sent by a reader impinges the antenna of a tag, the antenna interacts with the oscillating wave producing a high-frequency (RF) voltage. The voltage is rectified by a diode, and the resulting signal is smoothed using a storage capacitor to create a more-or-less constant voltage that is then used to power the tag's logic circuitry and memory access. There is also another rectification circuit with a smaller capacitance to allow the voltage to vary on the time scale of the reader data. This voltage is used to demodulate the information from the reader. This technique is known as envelope detection. Finally, to transmit information back to the reader, the tag changes the electrical characteristics of the antenna structure as to modify the signal reflected from it. Here, the field-effective transistor (FET) is used as a switch; when the FET is turned on, the antenna is grounded, allowing a large current to flow, and when it is off, the antenna floats allowing very little current [32 p. 36].

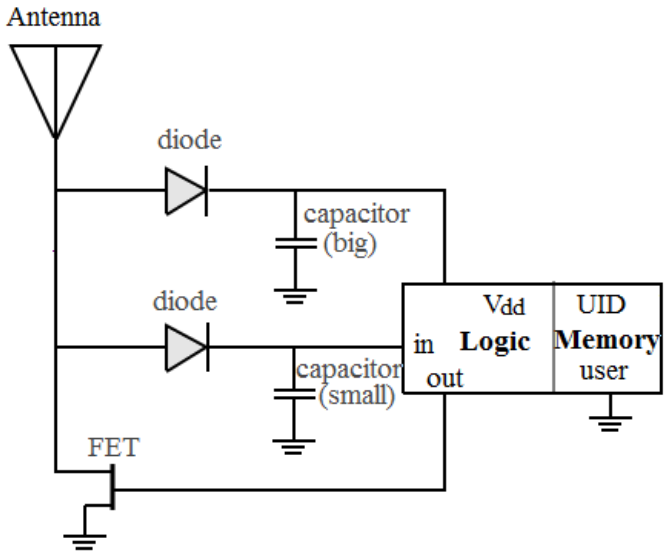

Figure 4.3. Schematic of simple passive RFID tag.

The advantage of passive tag is its simplicity, low cost, and no need for maintenance. But read range of passive tag is limited by the need to power up the circuitry, and so it is short compared to semi-passive tags. In passive tags computational power is minimized. So the readers must use very simple protocols to avoid overtaxing the tags, and integration of wireless sensors with the tags is challenging. This makes the security and privacy weakened due to the limited resources available to implement cryptographic algorithms, but this the security and privacy could be improved for HF tag if short read ranges are allowed [32 pp. 36-37].

4.3.2. RFID reader

A RFID reader is a radio transceiver. It contains a transmitter and a receiver that work together to communicate with the tag. So, a reader has the same challenges as all radios. The RFID reader has often one antenna which it uses in both transmission and reception. This is called a mono static configuration [32 p. 105]. The transmitter in the reader should have features as [32 p. 103]:

- Accuracy: it should be accurate in modulating the carrier frequency with the desired baseband signal and maintain the carrier at the desired frequency.
- Efficiency: the transmitter should deliver this signal at the desired absolute output power without excessive losses.
- Low spurious radiation: it should produce as clean and spur-free signal as possible with the amount of DC power available.
- Flexibility: the transmitter should turn off when it is not in use to save power and avoid producing large interfering signal. It should also turn on quickly when there are tags to be read.

The receiver in the reader should have feature as [32 pp. 103-104]:

- Sensitivity: the receiver must successfully receive and interpret very small signals. The ultimate limit of radio sensitivity is thermal noise.
- Selectivity: the receiver must detect the tag signal in the presence of often vastly more powerful interferers. For example, there might be many RFID readers working simultaneously, and signals from other readers might be much larger than the tag signal that should be read. In these situations the receiver should reject the signals outside the channel it is trying to receive, even if they are larger than the desired signal.
- Dynamic range: the receiver must be able to receive and interpret signals from tags at different distances. For instance a tag might be 3m away, or it might be 30 m away.
- Flexibility: in passive RFID protocols the transmitter transmits amplitude modulated signal and then it transmits CW signal when it awaits response from the tag. The receiver should recover quickly from any disturbance caused by the portion of the modulated signal that leaks into it, in order to hear the small tag response.

4.4. Effective aperture and radar cross section

As it is mentioned before, in a passive RFID system communication happens through modulation of the backscattering signal from the tag antenna. Thus, the operation of a passive RFID system has two principal limitations; the power transfer to the tag, and the power received by the reader. The first is described in terms of the effective aperture A_e, and the latter is described in terms of radar cross section σ of the tag antenna.

In order to derive equations for effective aperture and radar cross section, the tag is modelled as a series circuit, as shown in Figure 4.4.

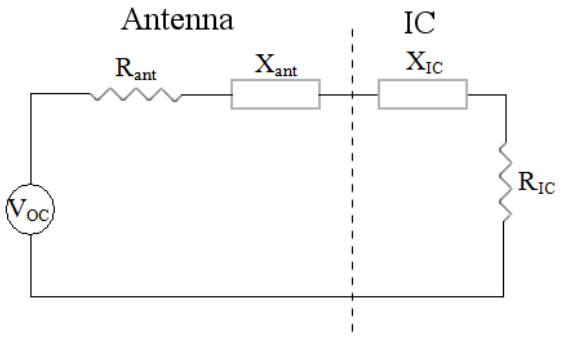

Figure 4.4. Circuit model of tag antenna and IC.

In the circuit model, the tag antenna is loaded by the IC's resistance and reactance. The effective aperture can be expressed in terms of the power dissipated in the load, while radar cross section can be defined in terms of the power dissipated in antenna resistance. The equations are the form [33 pp. 18-20]

$$A_e = \frac{\frac{1}{2}R_{IC}|I|^2}{S}, \quad (\mathrm{m}^2) \tag{4.1}$$

$$\sigma = \frac{\frac{1}{2}G_{tag}R_{ant}|I|^2}{S}, \quad (\mathrm{m}^2) \tag{4.2}$$

where I is the complex amplitude of the current in the circuit, the antenna gain G_{ant} accounts for the antenna losses and directivity when the scattered power is re-radiated, and S is the incident field power intensity, which is related to the voltage V.

Assuming maximum power transfer from the tag antenna to the IC, and defining current I in terms of voltage V, and antenna and IC impedances, the effective aperture and the radar cross section can be expressed as [33 pp. 18-20]

$$A_e = \frac{G_{tag}\lambda^2}{4\pi}\frac{4R_{ant}R_{IC}}{(R_{ant}+R_{IC})^2+(X_{ant}+X_{IC})^2} = \frac{G_{tag}\lambda^2}{4\pi}(1-|\Gamma|^2), \tag{4.3}$$

$$\sigma = \frac{G_{tag}^2\lambda^2}{4\pi}\frac{4R_{ant}^2}{(R_{ant}+R_{IC})^2+(X_{ant}+X_{IC})^2} = \frac{G_{tag}^2\lambda^2}{4\pi}|1-\Gamma|^2, \tag{4.4}$$

where Γ is the reflection coefficient. Equations consist of a maximum aperture (first fraction), and a second fraction describing the mismatch between the antenna and the load (IC).

In a conjugate match, i.e. for $\Gamma = 0$, the expressions (4.3) and (4.4) reduce to well-known aperture equations [33 pp. 18-20]

$$A_e = \frac{G_{tag}\lambda^2}{4\pi}, \tag{4.5}$$

$$\sigma = \frac{G_{tag}^2\lambda^2}{4\pi} = G_{tag}A_e. \tag{4.6}$$

4.4.1. Effect of modulation

Transferring data from the tag IC to the reader (uplink) requires a modulation between two impedance states Z_1 and Z_2, or reflection coefficients Γ_1 and Γ_2. The power available to the transponder is the average of the powers in each individual load state. Thus, the effective aperture and radar cross sections can be written as follows [33 pp. 20-23]

$$A_e^m = \frac{G_{tag}\lambda^2}{4\pi}\left(1-\frac{1}{2}[|\Gamma_1|^2+|\Gamma_2|^2]\right), \tag{4.7}$$

$$\sigma^m = \sigma_0+\sigma_m = \frac{G_{tag}^2\lambda^2}{4\pi}\left|1-\frac{1}{2}(\Gamma_1+\Gamma_2)\right|^2 + \frac{G_{tag}^2\lambda^2}{16\pi}|\Gamma_1+\Gamma_2|^2, \tag{4.8}$$

where the subscript *m* denotes the modulated state. The first term of radar cross section, σ_0, describes scattering at the carrier frequency, and the term σ_m describes scattering hat carries information at the sideband frequencies.

Equations (4.7) and (4.8) are not for a specific type of load modulation. The reflection coefficient determines describe modulation in terms of the transferred and scattered power. In general, the tag IC modulated both the amplitude and the phase of the scattered signal. For example a modulation of the load resistance with states $\Gamma_1 = -1$ and $\Gamma_2 = -1/2$, arises amplitude modulation, because the reflection coefficients have the same phase but different magnitudes. On the other hand states $\Gamma_1 = -1$ and $\Gamma_2 = 1$, arise phase modulation [33 p. 23].

Usually a switched capacitor or a switched resistor modulator is used in the microchips. Hence, the scattered signal will include both phase and amplitude modulation. The reader needs quadrature downmixers to detect both amplitude and phase modulation, and also advanced algorithms are required for optimal detection [33 p. 23].

4.5. Link budgets

Link budget determines the amount of power that is needed to transmit a signal across a wireless link in order that the transmitted data successfully receives. Since both readers and tags sends signal, for RFID system there are two separate link budgets; one associated with the reader-to-tag communication (the forward link budget) and one with the tag-to-reader communication (the reverse link budget)[32 p. 74]. In general, a link budget equation looks like this:

Received Power (dBm) = Transmitted Power (dBm) + Gains (dB) − Losses (dB)

In the above equation decibels are logarithmic measurements, so adding decibels is equivalent to multiplying the actual numeric ratios.

First it is simpler to derive link budget equation for forward link of RFID system. In forward link the reader antenna transmits electromagnetic wave and the tag antenna receives a portion of this radiated power. The ratio of the amount of received power and transmitted power depend on the geometry of the antennas, on the gains of the antennas, on the distance between them, and on all the possible losses that exist in the path of the signal (path loss). The amount of collected power is proportional to the density of power impinging on the tag antenna and to the effective aperture A_e of the tag antenna. The incident power density *S* of an antenna is [32]

$$S = \frac{P_{TX} G_{TX}}{4\pi r^2}, \tag{4.9}$$

where P_{TX} is reader antenna's transmitted power, *r* is the distance between the reader and the tag, λ is the wavelength of the incident wave, and G_{TX} is gain of the reader an-

tenna. The gains G_{TX} is measured relative to an isotropic antenna, that is in dBi [32 p. 87].

Using this equation, we can derive a general equation for the power received by a receiving antenna (tag antenna) RX from a transmitting antenna TX, if both gains and the distance *r* between them are known. So, the received power is [32 p. 87]

$$P_{RX} = P_{TX}G_{TX}\frac{A_{e,RX}}{4\pi r^2} = P_{TX}G_{TX}G_{RX}\frac{\lambda^2/4\pi}{4\pi r^2} = P_{TX}G_{TX}G_{RX}\left(\frac{\lambda}{4\pi r}\right)^2. \quad (4.10)$$

The last form of equation is known as the Friis equation. As a consequence, Friis equation illustrates the forward link budget of RFID system.

Friis equation can be modified for the reverse link power transmission of RFID system. Defining backscatter transmission loss T_b, the equation for the backscattered power to the reader antenna, in other words, the received power by the reader antenna gets the form [32 p. 87]

$$P_{RX} = P_{TX}G_{TX}\frac{A_{e,RX}}{4\pi r^2} = P_{TX}G_{TX}G_{RX}\frac{\lambda^2/4\pi}{4\pi r^2} = P_{TX}G_{TX}G_{RX}\left(\frac{\lambda}{4\pi r}\right)^2. \quad (4.11)$$

$$P_{TX,tag} = P_{TX,reader}G_{reader}G_{tag}\left(\frac{\lambda}{4\pi r}\right)^2 T_b \quad (4.12)$$

$$\Rightarrow P_{RX,reader} = P_{TX,reader}T_b G_{reader}^2 G_{tag}^2\left(\frac{\lambda}{4\pi r}\right)^4. \quad (4.13)$$

Equation (4.13) is derived from equations (4.11) and (4.12), and it is the reverse link formula of RFID system [32 p. 87].

4.6. Tag antenna design

A tag antenna is a critical component in RFID system. Challenges in designing a tag antenna are different from challenges in the normal antenna's design. One of the most important challenges is decreasing the total cost of the tag. The total cost, including IC, substrate, antenna material, adhesive, die attach, and testing, must be less than US$1 for most applications [32 p. 305]. Additionally, the size of the tag should be appropriate to fit in labels in different applications. But in tag antenna design, the most important task is to match the antenna impedance to the IC load in order to have maximum power transfer between the antenna and the IC.

The Friis equation (4.10) defines the amount of power the tag antenna receives. But antenna terminals are connected to the IC with distinct impedance, and the tag antenna cannot necessary deliver all the received power to the IC. The tag antenna should be designed such that it could deliver the received power to the IC as perfectly as possible. In order to investigate power transfer between the tag antenna and the IC, we treat the tag antenna as a voltage source, which is connected to the IC through complex imped-

ance consisting of the radiation resistance R_{ant} and a reactance X_{ant} (Figure 4.4). Similarly, the IC is treated as complex load impedance.

The power transfer equation defines the ratio of the power delivered to the IC to the maximum power it could have received according to the Friis equation. The power transfer equation is [32 p. 310]

$$\tau = \frac{P_L}{P_{Friis}} = \frac{4R_{IC}R_{ant}}{|Z_{ant} + Z_{IC}|^2}, \tag{4.14}$$

where R_{ant} is the resistance of the tag antenna at its terminals, Z_{ant} is the impedance of the tag antenna at its terminals, R_{IC} is the input resistance of the IC, and Z_{IC} is the input impedance of the IC. The power transferred to the IC is maximized when $\tau = 1$. This is achieved when resistances R_{ant} and R_{IC} are the same, and reactances Z_{ant} and Z_{IC} has the same value but opposite signs. Hence, the tag antenna should be conjugate matched to the IC in order to have maximum power transfer to the IC [32]. In the power transfer equation it is assumed that the input impedance of the IC is linear and complex, but this is an approximation, because IC has nonlinear devices as diode. On the other hand, in the conjugate matching and in the power transfer equation, the impedance of the IC is taken into account only at the power level where the IC turns on (IC's sensitivity).

The power transfer coefficient is used in the definition of the antenna performance parameter, realized gain. So realized gain is a parameter that beside the directivity and the efficiency of the antenna, accounts for the impedance matching of the antenna and the IC. Consequently, realized gain is defined as

$$G_r = \tau G, \tag{4.15}$$

where G is gain of the antenna. Realized gain is also expressed in dBi.

4.7. Read range

One of the most important parameters that describe the performance of the tag antenna is the read range of the tag. Read range is the maximum distance of tag at which the reader manages to read the information stored in the tag IC. In other words, if the distance between the reader and the tag is longer than the read range, the tag is hided. The reason is that either the antenna does not receive enough power to turn on the IC, or the backscattered signal at the reader is not strong enough to be demodulated [31][32].

As it is mentioned before, the Friis equation (4.10) does not take into account the non-idealities related to the RFID system. It does not account for the impedance mismatch, and the existing losses (cable loss, polarization loss etc.). Thus, accounting for these non-ideality factors, the transmission equation can be written as

$$P_{ic,th} = \tau G_{tag} G_{tx} L \left(\frac{\lambda}{4\pi r}\right)^2 P_{th}, \tag{4.16}$$

where $P_{ic,th}$ is the sensitivity of the microchip, P_{th} is the equivalent transmitted threshold power that would be measured in the perfect empty space conditions, L is the cable loss (assuming that the RFID system is in free space, and reader and tag antennas are polarized matched) from the generator's output to the input port of the reader antenna, G_{tx} is gain of the reader antenna, and G_{tag} is tag's antenna gain, and r is the distance between the reader antenna and the tag antenna.

Consequently, from equation (4.15) the read range can be defined as

$$r = \frac{\lambda}{4\pi} \sqrt{\frac{\tau G_{tag} G_{tx} L P_{th}}{P_{ic,th}}}. \tag{4.17}$$

According to the above equation, read range is proportional to the transmitted power from the reader antenna. But reader's transmitted power cannot be increased limitlessly. There are regulatory limitations considered for the transmitted power. For example, in Europe an unlicensed transmitter is allowed to use up to 3.28 W (EIRP=3.28W). The limitations are presented as effective isotropic radiated power (EIRP) values. EIRP is a function of gain and transmitted power of an antenna, and it defines the amount of power that would be needed to put into an isotropic antenna to get the same peak power as we get in the main beam of a directional antenna. Mathematically, EIRP is

$$EIRP = P_{tx} G_{tx}. \tag{4.18}$$

Using the EIRP value, and assuming zero loss in simulation environment, the simulated read range can be defined as

$$r_s = \frac{\lambda}{4\pi} \sqrt{\frac{\tau G_{fwd} EIRP}{P_{ic,th}}}, \tag{4.19}$$

where G_{fwd} is tag antenna gain in the forward direction. On the other hand, in the measurement environment the read range value is defined based on the peak power of the main beam as

$$r_m = \frac{\lambda}{4\pi} \sqrt{\frac{EIRP}{L_{fwd} P_{th}}}, \tag{4.20}$$

where p_{th} is threshold power, and L_{fwd} is the forward loss factor. Equation (4.19) and (4.20) define the read range value achieved in the main beam direction of the reader antenna, when the reader- and tag antenna's polarizations are matched.

4.7.1. Dipoles

A dipole yields a convenient starting point to tag antenna design. Usually in the design we start with a half wavelength dipole, which is shown in Figure (4.5). The dipole is at resonance when it has a length of $\lambda/2$ (at f=915 MHz, l=16 cm), which means that the reactance of it is approximately zero. On the other hand, the IC is capacitive and only an inductive antenna can conjugate match to the IC. In consequence, the dipole should be modified to achieve an inductive reactance and an appropriate resistance to maximize the power transfer [32 pp. 314-315]. In other words, the dipole should be designed such that it stores more energy in its magnetic field in order to increase the inductance of it.

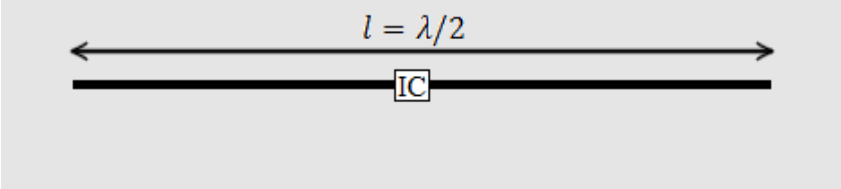

Figure 4.5. Half-wave dipole as a tag antenna.

There are numerous ways to increase the inductance of a dipole. For instance increasing the length of a half-wavelength dipole makes it inductive. But in most applications, a tag antenna should be smaller than 100 mm to fit in a label, and even 16 cm is too long for a tag antenna. This problem can be solved by bending the dipole (planar), which increases the length of the dipole and makes the total size of the antenna smaller. A meandered dipole is resulted when more bends are added. Meandering is not the only solution to match the antenna impedance to the IC impedance. We can also add matching elements to the antenna structure. One of the most used matching networks in tag antenna design is a T-match network [32 p. 315].

T-match consists of a dipole of length $a \leq l$ connected to the main dipole at a distance b. Figure 4.6 shows the geometry of a planar dipole with a T-match network and the equivalent circuit.

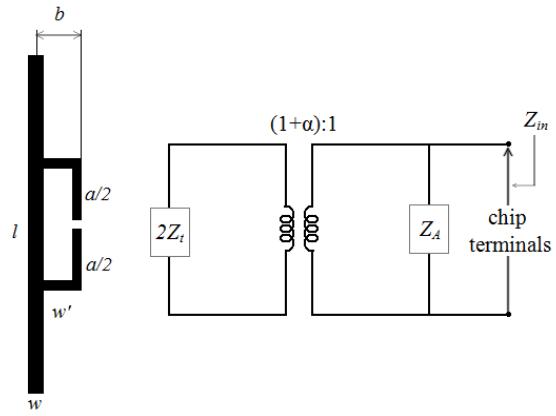

Figure 4.6. T-match configuration for planar dipoles, and the equivalent circuit.

As shown in Figure 4.6 the T-matching circuit acts as transformer and matches the antenna impedance to the chip impedance through the adjustment of a new degree of freedom, the parameter α. It can be proved that the antenna impedance at its terminals is given by [17 pp. 531-532]

$$r_s = \frac{\lambda}{4\pi}\sqrt{\frac{\tau G_{fwd} EIRP}{P_{ic,th}}}, \tag{4.21}$$

where $Z_t = jZ_0 \tan ka/2$ is the input impedance of the short-circuit stub formed by the T-match conductors and part of the dipole, Z_A is the dipole impedance taken at its centre in the absence of the T-match connection. Z_t depends on Z_0, which in turn has an equation of $Z_0 \cong 276 \log_{10}\left(b/\sqrt{r_r r_e'}\right)$. Z_0 is the characteristic impedance of the two-conductor transmission line with spacing b; $r_e = 0.25w$ and $r_e' = 8.25w'$ are the equivalent radii of the dipole and of the matching stub that are supposed to be planar traces; and $\alpha = \ln(b/r_e')/\ln(b/r_e)$ is the current division factor between the two conductors [17 pp. 531-532].

The dimensions of the T-match and the trace width *w'* can be adjusted to match the antenna impedance to the chip impedance. For the case of half-wavelength dipoles the resulting input impedance is inductive, while for smaller dipoles the total input impedance can be both inductive and capacitive [34].

5. WEARABLE ANTENNAS AND THEIR MANUFACTURING TECHNIQUES

Body-centric wireless communication has an important part of fourth generation mobile communication system (4G). Body-centric communications are related to personal area networks (PANs) and body-area networks (BANs). There are three kinds of body-centric communication applications; on-body communications, off-body communications, and in-body communications. On-body communication describes the link between body mounted devices communicating wirelessly. In-body communication is communication between wireless medical implants and on-body nodes. Finally, off-body communications defines the radio link between body-worn devices and base units or mobile devices located in surrounding environment [35]. Wearable RFID tags can be used in off-body communication applications.

Wireless off-body communication can be used in applications such as wireless sensor systems in security, healthcare and biomedical applications. Also, they can be applied for the purpose of monitoring of, for example, youngsters, the aged, and athletes. The off-body communication applications require development of wearable antennas that are mechanically robust, reliable, light weight, low cost, and almost maintenance-free. In addition, it is preferable that the wearable antennas do not need installation. In most applications the wearable antennas should also be integrated into the clothing seamlessly.

Wearable antennas have been designed for WLAN, GPS, and military related applications in [3], [4], [5], and [6]. There have been used flexible substrates such as elastic polymers and fabrics. For the radiating element of antennas, they have used conductive textiles and conductive threads. Also, a few wearable RFID tags have been designed in [7], [9], and [10]. In the mentioned articles, the authors have sewed different RFID tag antennas on textile, using different kinds of conductive threads. Also in this project, sewing is used as the manufacturing technique of RFID tag antennas. This chapter will introduce a few manufacturing techniques for wearable antennas.

5.1. Manufacturing techniques of wearable antennas

As it is mentioned before, wearable antennas should be light weight and have flexible substrates and conductive elements. Wearable antennas often include elastic polymers and fabrics as substrates and metallic composites as conductors. Several conductive materials have been reported in literature, including fibers having polymer cores and metallic coatings (E-fibers) [36][37], yarns bundled with thin metal filaments,

yarns/fabrics embedded with carbon nanotubes [38], and fabrics embedded with metal filaments [39].

In [38] the authors have designed and fabricated a conformal and lightweight patch antenna made of polymer-ceramic composites as the substrate, and E-textile as conductor operating at 2 GHz. The polymer-ceramic composites are highly flexible, low cost, lightweight and low-temperature handling materials suitable for RF applications. With proportional mixture of ST ceramic powder with Polydimethylsiloxane (PDMS), dielectric permittivity ranging from 3 to 13 with a loss tangent of less than 0.01 can be achieved [38]. The authors have fabricated E-textile by coating a textile with SWNTs (single-walled carbon nanotubes) and Au particles to improve the conductivity (Figure 5.1 (a)). The E-textile is then embedded on a polymer-ceramic (PDMS and SrTiO3) composite. To embed the E-textile to the substrate, they first patterned the textile according to the planar antenna geometry specifications (Figure 5.1 (b)). Then, they mixed the polymer-ceramic composite over the E-textile fabric (Figure 5.1 (c)), and waited for 12 hours for curing. According to their test results conductive textile adheres strongly to the polymer-ceramic composite. The final configuration was a flexible patch antenna, shown in Figure 5.1 (d) [38].

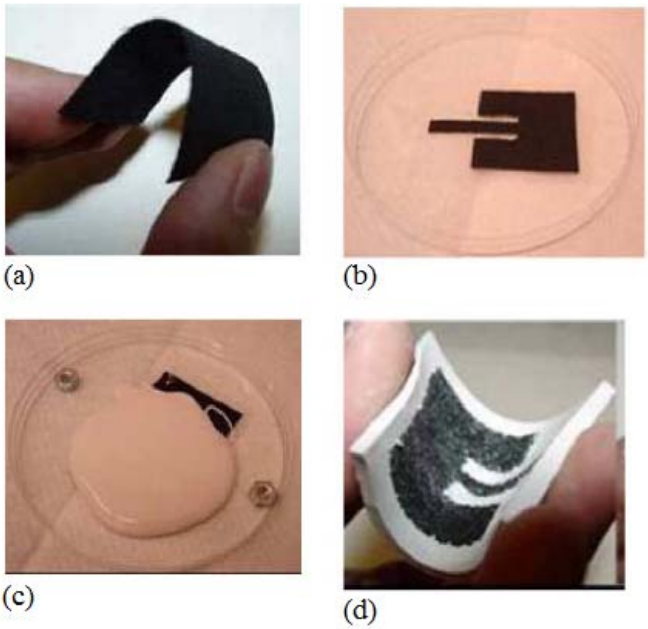

Figure 5.1. (a) E-textile, (b) E-textile cut based on planar antenna dimensions, (c) E-textile mix with polymer composite, (d) Final form of the antenna after several hours of curing [38].

The fabricated patch antenna has a gain of 6 dB at 2 GHz, which is 2 dB less than that of an ideal patch with the same dimensions and lossless materials [38].

The substrate, PDMS, is also used in [36], [40], and [41] in fabricating different patch antenna configurations and microstrip lines. However, the authors of these articles have used embroidered E-fibers on reinforcing textiles as the radiating elements of the antennas. Then, they have assembled the embroidered E-fibers/textile with the PDMS

substrate to form a RF functional element. According to all these articles, conductivity of embroidered E-fiber pattern is higher the higher the stitching density is and the neater the fabricated pattern is.

In [3], [4], and [5], authors have designed flexible, lightweight WLAN and GPS antennas consisting of fabrics as substrate and conductive textiles as radiating element of the antenna. In all the presented articles, the authors have designed flexible antennas that have a ground plane which minimizes the effect of human body on the operation of the antenna. But, most RFID tag antennas do not have a ground plane. Additionally, a wearable RFID tag should be small and seamlessly integrated into the clothes.

The authors of articles [7] and [10] have designed embroidery RFID tag antennas. In their prototypes the tag antenna shapes are sewed on the textile (substrate) using conductive threads. They have explored the effect of the choice of the conductive thread, the effect of stitch density and the sewed pattern, and the effect of the direction of the stitches on the conductivity of the sewed structure. According to [7] and [10], the conductivity improves as the number of stitches increases. Additionally, according to the article [10], sewing method (sewing direction) affect the conductivity too. For an RFID tag, sewing the antenna geometry on a textile which can be used in clothing is a very good, if not the best, manufacturing technique, because in this way the tag will be embedded into the clothing in different shapes (for instance, in the shape of logo of a company, or a letter shape [7]) seamlessly.

6. SIMULATION OF AN RFID DIPOLE

The objective of this project was to investigate the operation of sewed dipoles on cotton as substrate. First, the optimum geometry of a dipole, operating in the UHF RFID region, had to be defined. This is done using ANSOFT's High Frequency Structure Simulator (HFSS), which is a numerical solver of electromagnetic wave equations based on the finite element technique.

Factors that define the operation of an RFID tag antenna are the substrate and the geometry of the planar antenna, which in turn depends on the conductivity and the thickness of the metal structure. The conductivity of the conductive thread and the electrical properties of cotton were unknown. So, electrical properties of cotton are defined, and the process is explained in detail in Section 6.1. But defining the conductivity of a sewed structure is not straightforward, because in this case conductivity depends greatly on sewing method and sewing density [10], [7]. So, for the beginning, a copper dipole was designed in order to find an optimum geometry for a planar dipole operating in the UHF region. Section 6.2 explains simulation of this antenna using cotton as the substrate.

6.1. Determination of electrical properties of fabric

Dielectric constant of cotton is measured using the resonance method discussed in detail in [8]. In this method the dielectric of the fabric is measured when the fabric is as the substrate of a microstrip radiator, while the ground plane and the patch are made of copper.

First, a patch antenna is designed with HFSS simulator using approximate dielectric constant and loss tangent values. A special care has been taken that the area of the ground plane and the fabric would be at least five times larger than that of the rectangular patch, in order to avoid backlobes in the radiation pattern of the antenna, reduce the diffraction and scattering effects at the edges on the ground plane, and also to minimize the undesirable effects of surface waves [8]. The structure of the designed patch antenna is shown in Figure 6.1. The thickness of cotton is measured as 0.25mm, and the thickness of copper tape is 0.05mm.

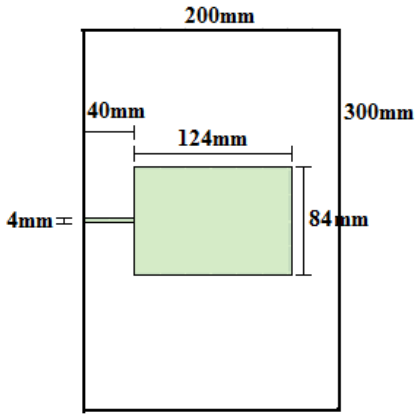

Figure 6.1. Geometry of one of the patch antennas used in determining the electrical properties of cotton.

After the design process, the patch antenna is manufactured and its resonance frequency is measured using a vector network analyser. Then, in the HFSS model, the permittivity of the substrate was set as a sweep parameter to find the permittivity value that results the same resonance frequency as the measured resonance frequency.

This method is used to find the permittivity and loss tangent of cotton for four different patch antennas. The resulted relative permittivity values vary from 1.77 to 1.83. In this project it is used 1.8 as the relative permittivity of the cotton. In addition, the found loss tangent is approximately 0.018.

6.2. Simulation of a copper dipole on textile

The structure of the designed dipole is shown in Figure 6.2 with the detail of dimensions. The dipole is designed for Alien Higgs-3 UHF RFID IC [42] for an operating frequency of 867MHz. As Figure 6.2 shows, the input impedance of the dipole is matched to the chip input impedance using a T-match network. The thickness of the substrate (cotton) is 0.25mm, and the thickness of the copper is 0.05mm.

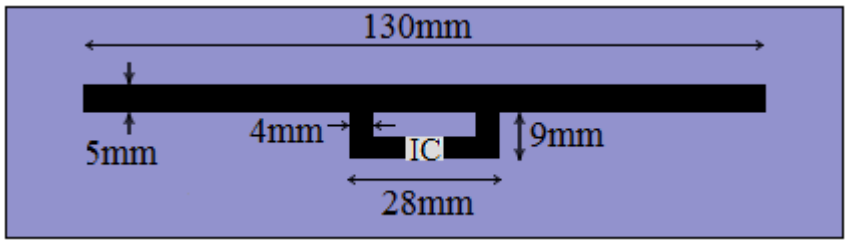

Figure 6.2. Geometry of the designed dipole-type tag antenna.

The designed tag antenna is then fabricated and measured in an anechoic chamber using Voyantic Tagformance RFID measurement system [43]. Figure 6.3 shows the simulated and measured realized gain graphs.

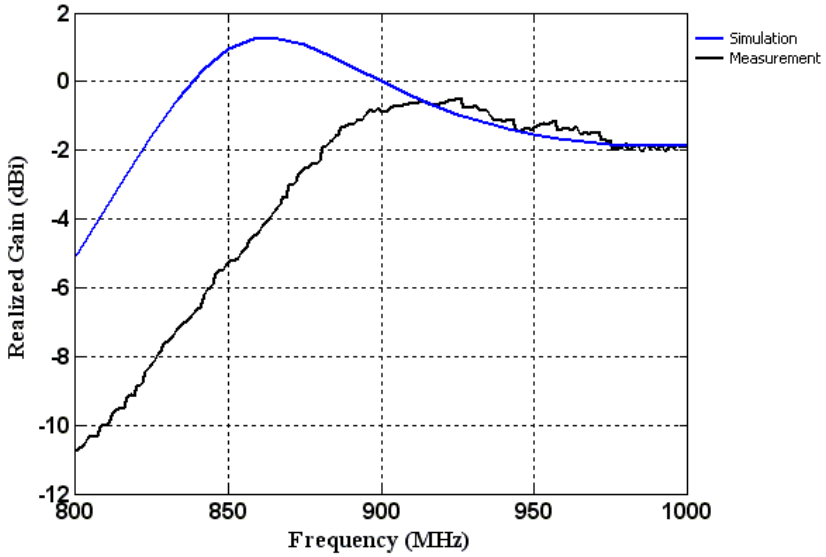

Figure 6.3. Simulated and measured realized gain of copper dipole tag antenna on textile.

The simulation and measurement results differ at frequencies less than 900 MHz. The reason for this difference is investigated by simulating and manufacturing a dipole on well defined substrate, Rogers RT/Duroid 5880 [44], with exactly the same geometry than the manufactured dipole on textile. Figure 6.4 shows the measurement and simulation results of the dipole on Rogers.

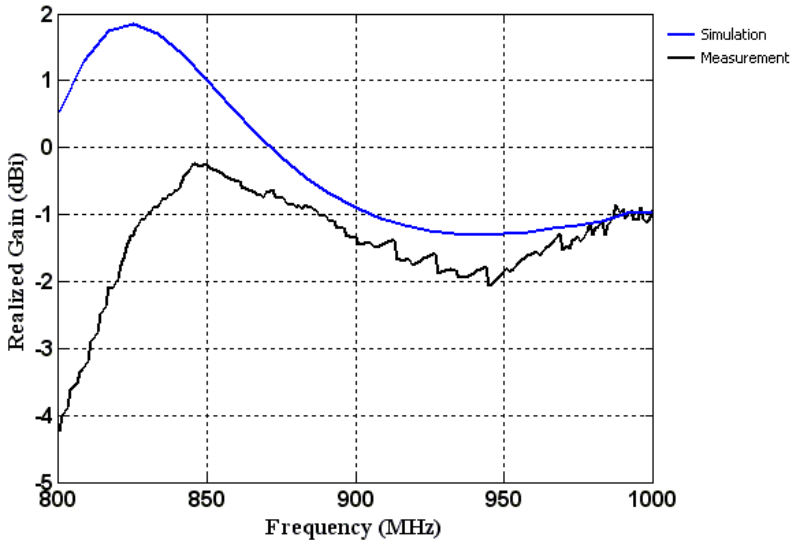

Figure 6.4. Simulated and measured realized gain of copper dipole tag antenna on Rogers.

In this case, simulation and measurement results match well at frequencies higher than 850 MHz. The circuit model of the chip used in simulations is defined for frequen-

cies higher than 860 MHz, which explains the difference of measurement and simulations results of the dipole on Rogers at low frequencies.

In consequence, only the fabric can cause the mismatch of the simulation and measurement results of the dipole on textile. In the HFSS model, the fabric is defined as a rigid body, but in reality textile is not rigid. This might be one of the differences between the reality and the HFSS model.

7. SEWED DIPOLES

The dipole, which is designed for copper and cotton as substrate, is sewed with Husqvarna VIKING computer aided sewing machine, using electric-thread 110f34 dtex 2-ply HC [45]. The thread has a weight of 110 dtex (dtex = g/10000m) raw yarn twisted with a second 110 dtex raw yarn to make a yarn of 220 dtex. Then the yarn is plated with silver to gain a weight of 275 dtex. The DC lineal resistivity of the thread is 500 ± 100 Ω/m, and the diameter is approximately 0.16mm. This is a multifilament thread, since it has 34 filaments in a yarn.

When an RFID tag antenna is designed, the conductivity of the electro thread has to be considered. There is not a straightforward way to calculate the conductivity of an electric thread. Usually we have to estimate the conductivity by doing some measurements. We cannot use equations (3.10) and (3.11) to calculate the conductivity of a conductive thread, because these equations are for a uniform metal rod with a uniform current distribution. But, conductive threads do not have a uniform metal structure, and they consist of many copper coated filaments. However, it is obvious that the conductivity of the thread is higher the higher the weight of the metal part of the thread is. For instance, the weight of silver in the thread we have used is 55 g/10000m (dtex), which provides a good conductivity. So, it is sufficient that the dtex value of the thread is high enough while the exact conductivity value of the thread is less important.

In practice, in order to make an efficient design of embroidered tag antennas with electromagnetic simulators, we can treat the complex embroidery pattern as a uniform conductive material layer when the electric threads are located densely [10][46]. Hence, it is the conductivity of an embroidery pattern that is an effective factor in the simulation model of an embroidery antenna. On the other hand, the conductivity of an embroidery pattern is different depending on the thread density and the sewing structure [10] [11].

This chapter discusses about dipoles sewed with two different sewing structures and with different stitch densities. The performance of the sewed tag in each case is measured and investigated. In addition, the conductivities of sewed tags are found using measurement results.

7.1. Vertically sewed dipoles

Conductivity of electrically conductive part of an antenna does not affect the operation frequency of the antenna directly. According to the equation (3.16) it affects only the quality factor of the antenna, and hence, it affects the frequency bandwidth of the antenna. According to the equation (3.16) a decrease in the conductivity results in an in-

crease in conductive losses, and thus a decrease in quality factor. On the other hand, a decreasing quality factor increases the frequency bandwidth of the antenna. On the basis of this explanation we can use the geometry of the designed copper dipole tag antenna for sewing tag antennas using an embroidery machine, because the dominant difference between copper and a sewed structure is the conductivity of them.

Consequently, the geometry of the designed copper dipole tag antenna is sewed using the embroidery machine Husqvarna Viking. The sewing pattern is selected with 5D Embroidery System software, and then it is sewed on cotton. The pattern consists of a horizontal line sewed along the dipole length, and zigzags sewed vertically on it. The effect of stitch and zigzag densities on the performance of the antenna is investigated by sewing 6 dipoles with different zigzag densities and measuring them in an anechoic chamber. The measurement results are presented and discussed in section 7.1.1.

In section 7.1.2, the simulation model of the vertically sewed tag dipoles are presented and discussed in detail. The simulation model presented in section 7.1.2 is then verified by comparing simulation and measurement results of 7 vertically sewed dipoles of different lengths.

7.1.1. Vertically sewed dipoles with different stitch densities

According to the articles [10] and [11] the conductivity of sewed structure increases as the thread density increases. In our case this means that increasing the zigzag density should increase the conductivity of the antenna. This is investigated by sewing dipole with six different zigzag densities, and measuring them. Sewed tags are shown in Figure 7.1 (a). Figure 7.1 (b) shows the measured forward read range graphs of sewed tags ordered by the amount of stitches. The dipole with 2550 stitches has the highest zigzag density, and the dipole with 225 stitches has the lowest zigzag density.

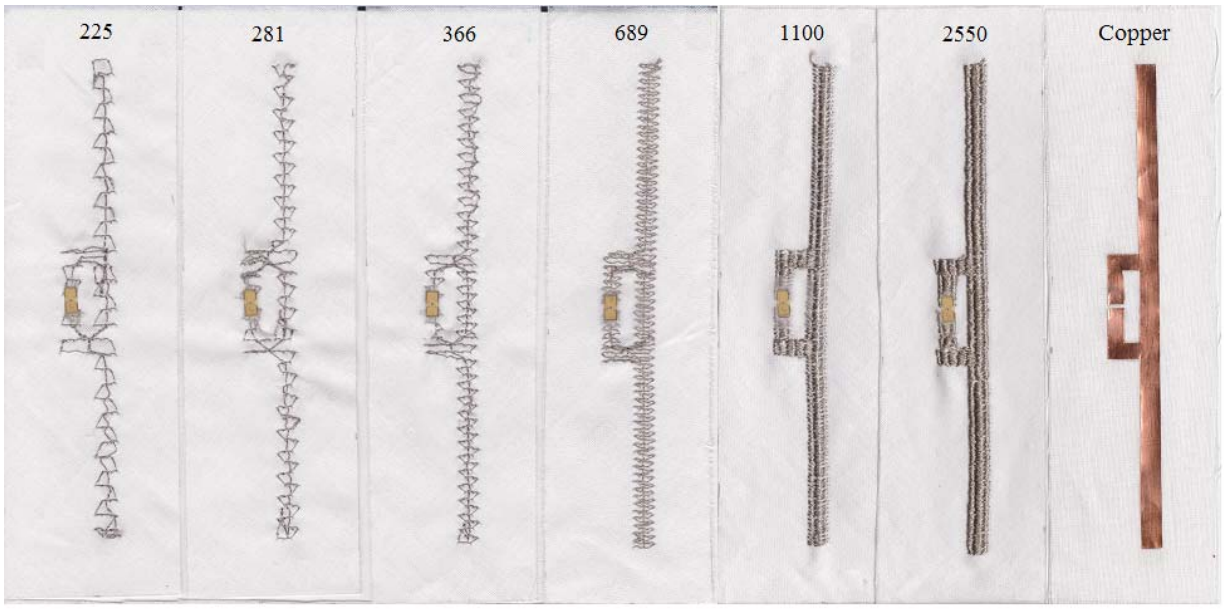

(a)

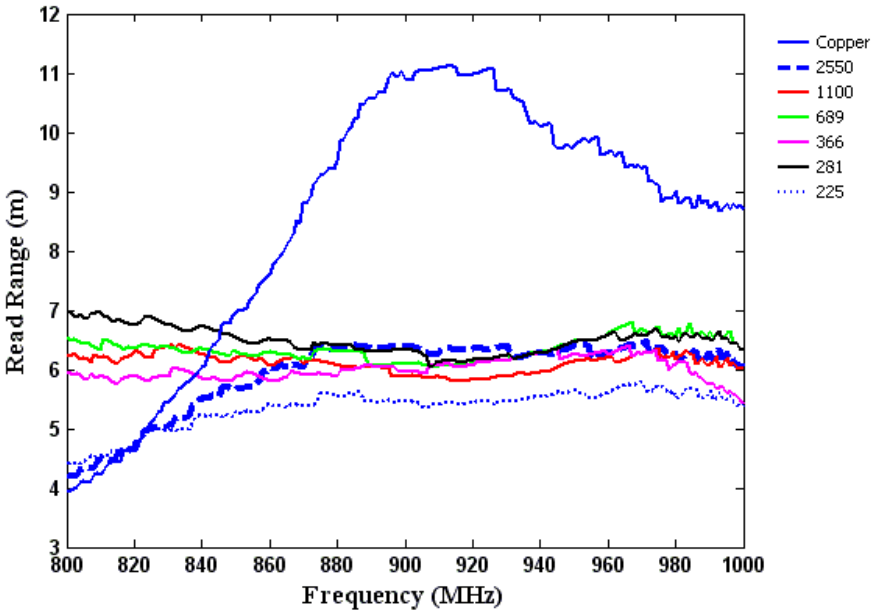

(b)

Figure 7.1. (a) Sewed tags with different stitch densities, (b) measured forward read range graphs of sewed dipoles with different stitch densities.

As Figure 7.1 (b) shows, vertically sewed tags have a wide frequency bandwidth, which is caused mainly by reduction of quality factor of antenna due to reduced conductivity of antenna. Figure 7.1 (b) also shows measured read range graph of copper tag antenna for comparing the performance of sewed antennas with the copper antenna.

From sewed tags we can achieve up to 7 m forward read range, which is a really good performance. According to this measurement results the performance of sewed tags does not change much in the function of sewing density, and only when the amount of stitches reduced from 281 to 225 the change of performance is visible. Consequently, we can sew antennas sparsely using less conductive threads and spending considerably less time for sewing, and still achieve as good performance as sewed antennas' with high density.

7.1.2. Modelling of vertically sewed dipoles

In the design of an RFID tag antenna the electrical characteristics of the electrically conductive part of antenna should be known. As it is mentioned before, electrically a sewed antenna can roughly be treated as a uniform metal structure with a distinct conductivity.

To find out the conductivity of vertically sewed structure the measured realized gain graphs of vertically sewed antennas are compared with simulation results of the dipole with different conductivity values.

As it can be seen from Figure 7.1 (a), the thickness of the sewed part changes as a function of stitch density. When the stitch and thread densities of a sewed structure are high enough, in a sense that the sewed structure resembles a flat structure, we can talk about the thickness of the sewed structure. But, when the sewed pattern is sparse, it is not convenient to talk about the thickness of a sewed structure, because the sewed structure is not flat and rigid. But still, in simulator we have to define a thickness for the antenna material. Thus, the thickness of the sewed structure on the upper face of each tag is measured, and it is set as the thickness of the conductive part of the antenna in HFSS simulator. The thicknesses of sewed planar dipoles are listed in Table 7.1.

Table 7.1. Thickness of the sewed structure on the upper face of each tag.

Stitch number	2550	1100, 689	366, 281, 225
Thickness (mm)	0.425	0.2	0.1

As it is illustrated in Figure 7.1 (b), the read range graphs of sewed dipoles are located closely to each other. From that graph we might conclude that the conductivities of sewed antennas are almost the same too. But when we consider the thickness of sewed structure we end up with different conductivity values for each of them. Figure 7.2 shows simulation result of the dipole with a thickness of 0.425mm, and measurement result of the sewed dipole with 2550 stitches. According to Figure 7.2, the conductivity of vertically sewed dipole with 2550 stitches is 2000 S/m.

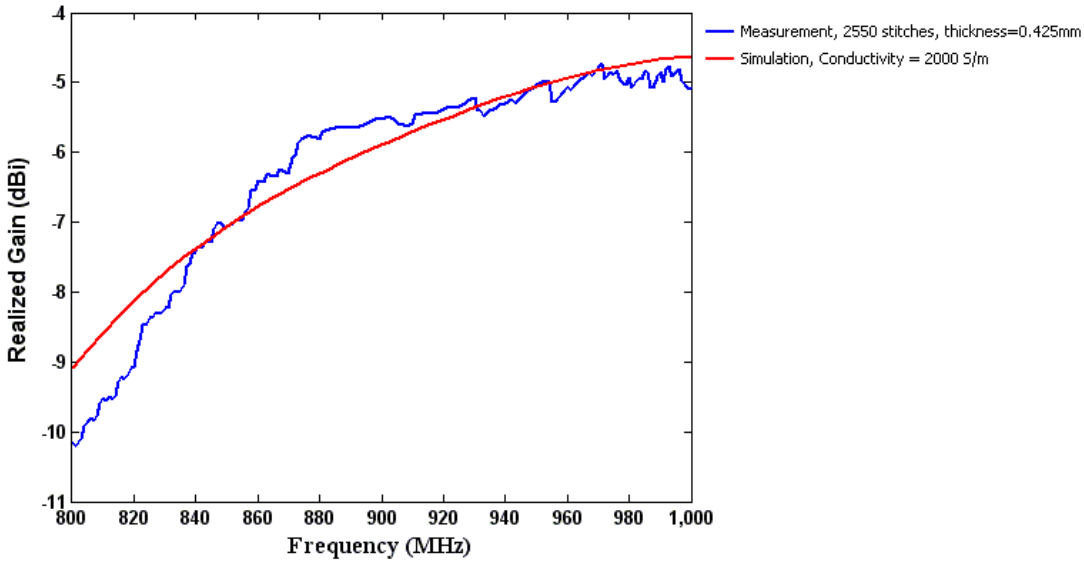

Figure 7.2. Measured realized gain of the sewed dipole with a stitch number of 2550, and simulated realized gain of the dipole with a thickness of 0.425 mm, and a conductivity of 2000 S/m.

Figure 7.3 shows simulated realized gain of the dipole with different conductivities, and measured realized gain of sewed dipoles with 1100 and 689 stitches. In this case, in

simulations the thickness of the dipoles is set as 0.2 mm. According to Figure 7.3, the conductivity of sewed dipoles with 1100 and 689 stitches varies from 3000 S/m to 5000 S/m.

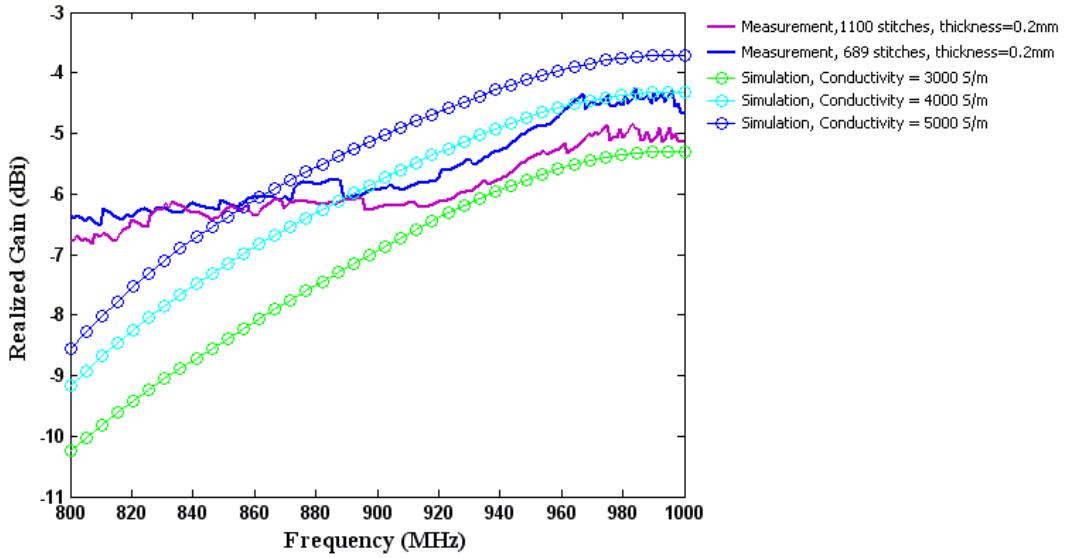

Figure 7.3. Measured realized gain graphs of sewed dipoles (with 1100 and 689 stitches) and simulated realized gain graphs of a 0.2 mm thick dipole for different conductivities.

Figure 7.4 shows simulation results and measurement results of sewed tag antennas with 366, 281 and 255 stitches. In this case, in HFSS model the thickness of the dipole is 0.1mm, which causes higher conductivity values than before. According to this figure the conductivity of these tag antennas varies from 6000 S/m to 9000 S/m.

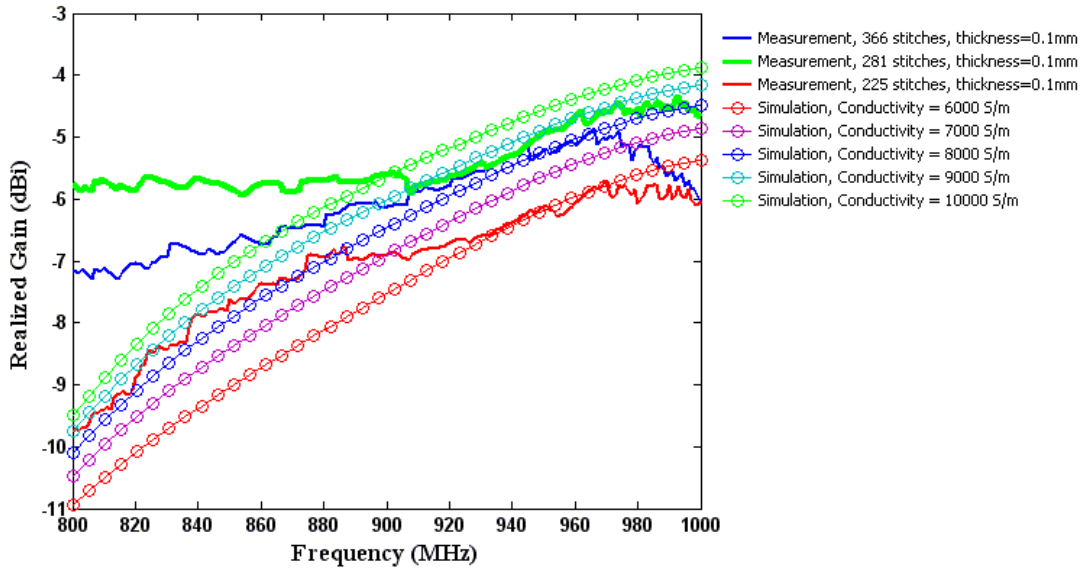

Figure 7.4. Measured realized gain graphs of sewed dipoles (with 366, 281 and 225 stitches) and simulated realized gain graphs of a 0.1 mm thick dipole for different conductivities.

In consequence, by comparing measurement and simulation results we can see that the conductivity of vertically sewed tag antennas varies from 2000 S/m to 9000 S/m depending on the zigzag density and the thickness of the sewed structure. According to the presented results, conductivity of the sewed dipoles decreases as the thread density and the thickness of the sewed pattern increases. There is little performance deviation between the sewed dipoles with 281-2550 stitches (Figure 7.1), while they have different thicknesses. Consequently, the thicker conductive layer must have less conductivity in order to have losses at the same level with the thinner one.

7.1.3. Vertically sewed dipoles with different lengths

As Figures 7.3 and 7.4 illustrate, simulated graphs do not follow perfectly the measured graphs of vertically sewed dipoles. In order to verify the model presented in Section 7.1.2 for vertically sewed antennas, 6 dipoles with six different lengths are sewed and measured. The measurement results are then compared with the simulation results of these tag antennas. Sewed tags are shown in Figure 7.5.

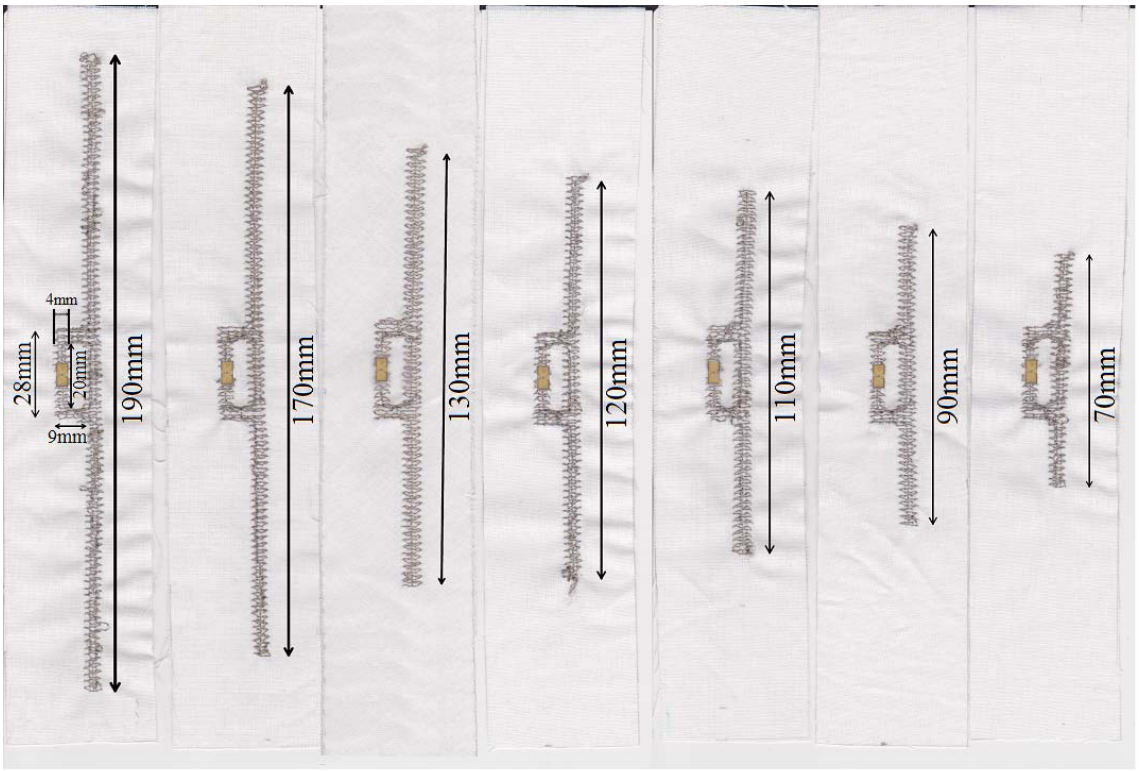

Figure 7.5. Sewed antennas with the same T-match geometryas before, but with different lengths.

The sewed dipoles have only different lengths, and other dimensions of them are maintained unchanged. These dipoles have the same zigzag density as the 130mm long dipole with 689 stitches. Consequently, the conductivity of them is 4000 S/m, and in all

of them the thickness of the sewed structure on the upper face of the tags is 0.2mm. These values are used in the HFSS models of them. Figure 7.6 shows the measured read range graphs, and Figure 7.7 shows the measured and simulated realized gain graphs.

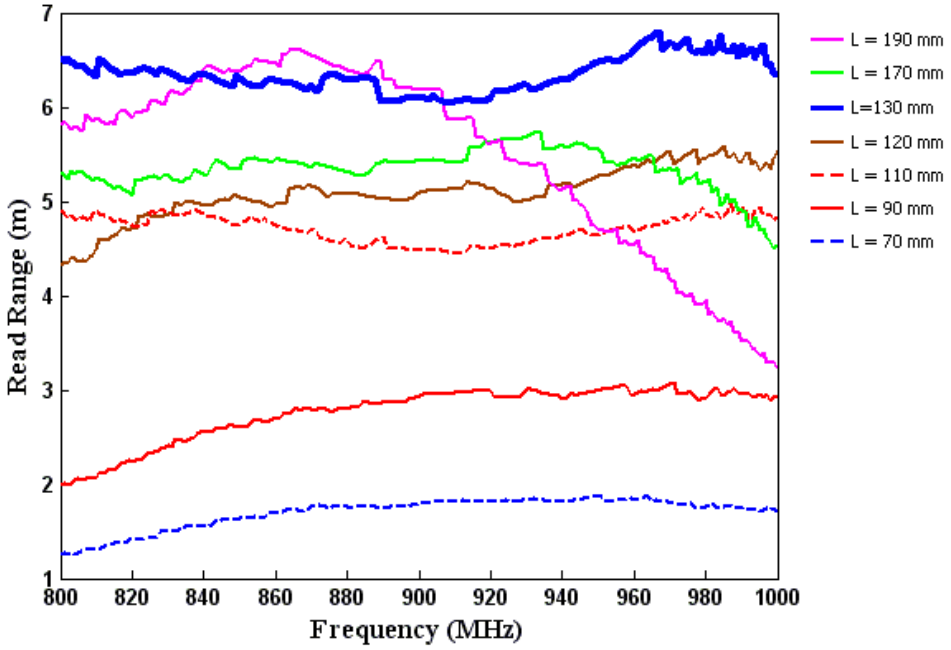

Figure 7.6. Measured read range graphs of sewed dipoles with different lengths.

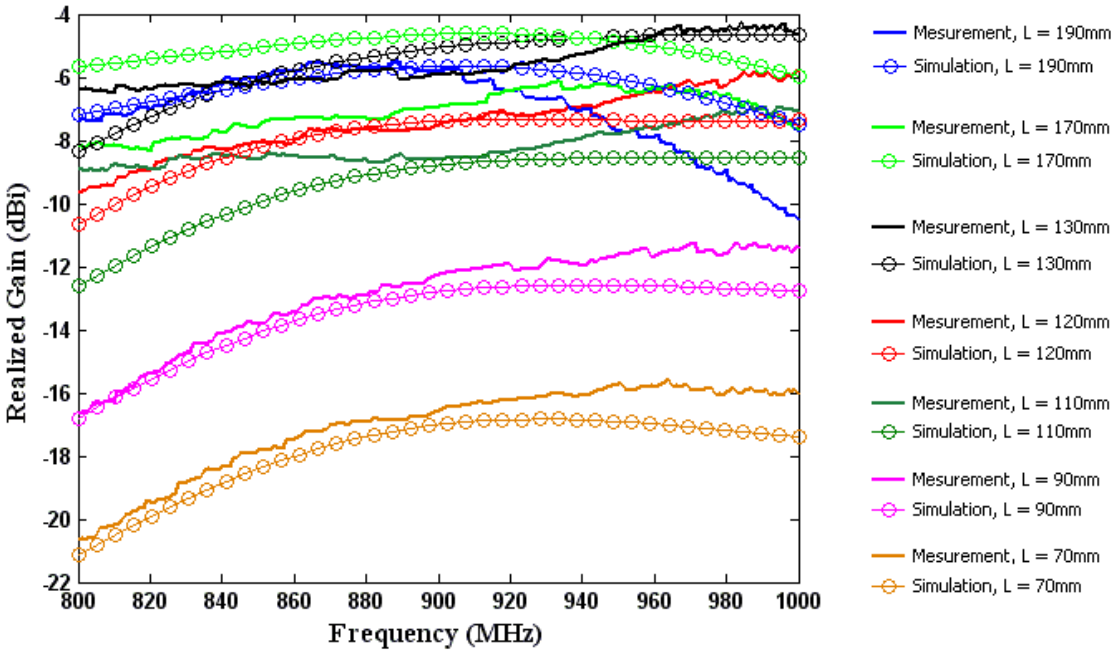

Figure 7.7. Measurement and simulation results of sewed dipoles with different lengths.

As Figure 7.7 shows, the measurement and simulation results of most of sewed dipoles match quite well. The reason for the slight difference in simulation and measurement results is that sewed antennas are not made of homogeneous conductive material as they are modelled in the simulator. Consequently, Figure 7.7 proves that the simulation model presented in Section 7.1.2 can be used in the design of embroidery tag antennas.

7.2. Horizontally sewed dipoles

According to the article [7] the sewing pattern affects the conductivity of the sewed antenna. In order to investigate the effect of sewing pattern of a dipole antenna on the performance of it, the geometry of the designed copper dipole tag antenna is sewed also with a horizontal pattern. In this case, the pattern consists of just horizontal lines along the length of the dipole. Also here, the effect of thread density in the sewed dipole structure is investigated by sewing two dipoles with two different thread densities; 869 and 506. The sewed dipoles are then measured, and their measurement results are compared with simulation results in order to find out the conductivity of them.

The horizontally sewed tags are shown in Figure 7.8 (a), and their measured read range graphs are presented in Figure 7.8 (b).

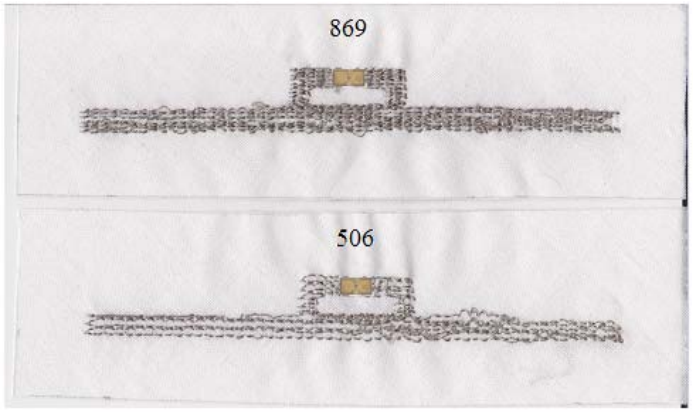

(a)

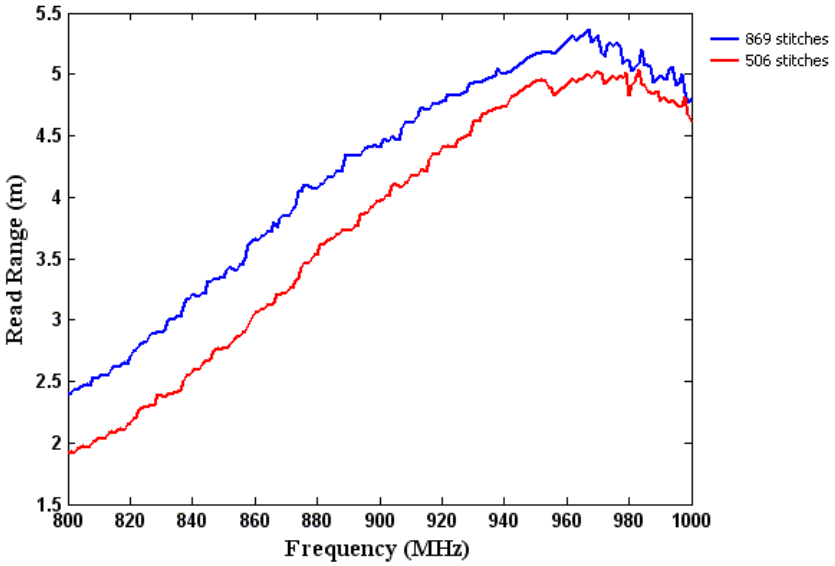

(b)

Figure 7.8. (a) Horizontally sewed dipoles, (b) Measured forward read range of sewed tags.

As Figure 7.8 (b) shows, read range values achieved with horizontally sewed tag antennas are smaller than the read range values achieved with the vertically sewed tag antennas. In addition, horizontally sewed tags are not as frequency wideband as vertically sewed tag antennas.

7.2.1. Conductivity of horizontally sewed dipoles

Conductivities of horizontally sewed dipoles are determined in a same way as the conductivity of vertically sewed dipoles. First, the thickness of the sewed part on the upper face of each sewed tag is measured. The thickness of the sewed tag with 869 stitches is approximately 0.2mm, and the thickness of the other one (506 stitches) is approximately 0.1mm. The geometry of each sewed dipole is then simulated with different conductivity values to see which simulated graph matches the measured graph the best. Figure 7.9 (a) shows the measured realized gain graph of the sewed dipole with 869 stitches, and the simulated realized gain of the dipole with a thickness of 0.2 mm. Likewise, Figure 7.9 (b) shows the measured realized gain graph of the sewed dipole with 506 stitches, and the simulated realized gain of the dipole with a thickness of 0.1 mm.

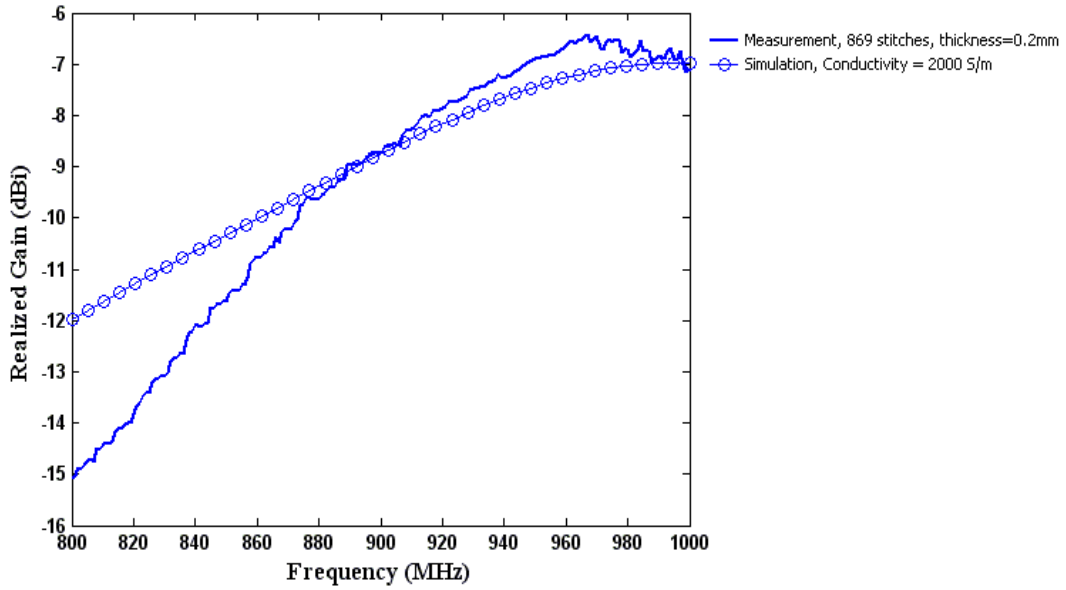

(a)

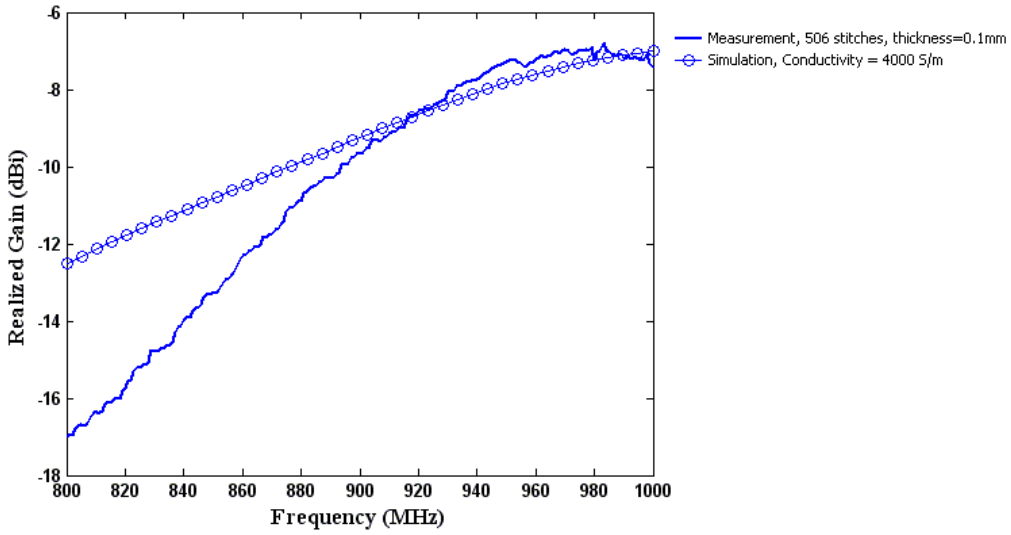

(b)

Figure 7.9 (a) Measured realized gain of horizontally sewed dipole 869 stitches and simulated realized gain of dipole with a thickness of 0.2mm, (b) Measured realized gain of horizontally sewed dipole with 506 stitches and simulated realized gain of dipole with a thickness of 0.1mm.

According to the Figure 7.9 (a) the conductivity of the horizontally sewed dipole with 869 stitches is approximately 2000 S/m, and the conductivity of the horizontally sewed dipole 506 amount of stitches is 4000 S/m. Similar to the case of vertically sewed dipoles, the conductivity of horizontally sewed dipole decreases as the stitch and thread density increases.

7.3. Vertically and horizontally sewed simple dipoles

Authors of articles [7] and [11] have proved that conductivity improves, if the sewing pattern consists of sewed lines along the direction of current flow. But, according to previously presented measurement results the T-matched vertically sewed dipoles have higher conductivities and read ranges than the T-matched horizontally sewed dipoles, although the horizontally sewed pattern consists of sewed lines along the dipole length and in the direction of current flow.

The reason for this difference is investigated by sewing two identical simple dipoles with both horizontally and vertically sewing patterns. Figure 7.10 (a) shows the sewed dipoles, and Figure 7.10 (b) shows the measured read range graph of them.

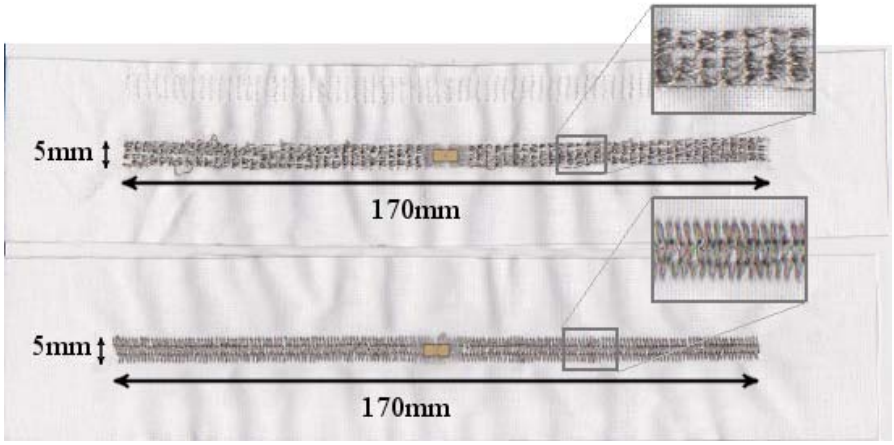

(a)

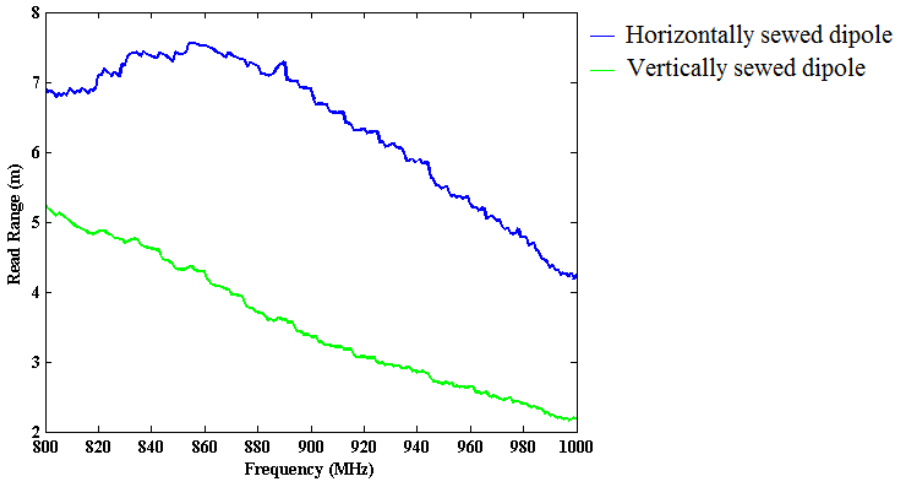

Figure 7.10 (a) Horizontally and vertically sewed dipoles, (b) Measurement results of the sewed dipoles.

As Figure 7.10 (b) illustrates, in the case of simple dipoles horizontally sewing pattern has better performance and higher conductivity than the vertically sewing pattern. This result correspond with the claim of authors of the articles [7] and [11], which states

that the conductivity increases if the sewing pattern consists of sewed lines in the direction of current flow.

Apparently, the reason for the weakened performance of T-matched horizontally sewed dipoles is the imperfect current flow in the vertical section of T-matching network. Consequently, in the design of embroidery antennas, we have to consider the direction of current flow in the whole antenna, and choose a sewing pattern which has conductive threads going along the current.

8. CONCLUSIONS

The aim of this project was to investigate and characterize the performance of sewed dipole-type RFID tag antennas, and develop models and methods to predict the antenna parameters of them. Along with the characteristics of substrate of an antenna, the conductivity of the radiating element is one of the determining factors in antenna design. In the case of sewed tag antennas, it is the conductivity of an embroidery pattern that is an effective factor in the simulation model, because the sewed pattern can be treated as a uniform metal structure. The relative positioning of electric threads in a sewing pattern might have influence on the input impedance of a sewed tag antenna. But, in this project we have neglected this aspect, because effect of the sewing pattern on conductivity dominates compared to the effect on impedance.

According to previous researches done in [7], [9], [10], and [11], the conductivity of an embroidery pattern depends on the selection of the conductive thread, the thread density and the sewing structure. In this project, the effect of these factors is investigated by manufacturing and measuring sewed dipole-type tag antennas with two different sewing patterns, and with different thread densities. The dipoles are sewed on cotton (ε_r = 1.8 and tan δ = 0.018) using electro-thread 110f34 dtex 2-ply HC. The conductivity of the sewed dipoles is then evaluated by comparing measurement results and simulation results.

First, a dipole-type RFID tag antenna has been designed for UHF RFID applications. Then the designed dipole is embroidered with two different patterns; horizontally sewing pattern, and vertically sewing pattern. The vertically sewed pattern consists of a sewed line along the length of the dipole, and zigzags sewed on it. But the horizontally sewed dipoles have just lines along the length of the dipole.

Vertically sewed dipole have read ranges varying from 6m to 7m at 900MHz, which is a really good performance compared with previously fabricated embroidery RFID tag antennas in [7], [9], [10]. Conductivity of vertically sewed dipoles varies from 2000 S/m to 9000 S/m depending on the zigzag density and the thickness of the sewed structure. Conductivity of the horizontally sewed dipole with 869 stitches is evaluated as approximately 2000 S/m, and the conductivity of the horizontally sewed dipole with 506 stitches is evaluated as 4000 S/m. According to the modeling technique presented in the thesis, the conductivity of sewed antennas decreases as the thread density and the thickness of sewed structure increases. On the other hand, according to the previously published articles related to sewed tag antennas, increasing the thread and stitch density results in an increase of the conductivity of a sewed structure. The reason for the different results of this thesis and the previous articles is that, in simulation model we have

considered, also, the thickness of the sewed antennas, while the authors of previously published articles did not consider this aspect.

According to the results of this project, we can conclude that the main difference between a sewed antenna and a copper antenna is their conductivity. In addition, each sewing pattern has its own conductivity, and when designing an embroidery antenna we have to find a pattern that has the best conductivity. Conductivity of a sewing pattern improves if the pattern consists of sewed lines along the direction of current flow. It is not necessary to sew the chosen pattern with a high thread density. We can achieve high conductivities even from very sparsely sewed antennas, using less conductive threads and spending considerably less time on sewing.

The evaluated conductivities of the sewed dipoles and the presented simulation model of them can be used in future for optimization of the sewed antennas to operate in the vicinity of body.

In future, the operation of sewed tag antennas can be explored more precisely by studying the effect of relative positioning of electric threads in a sewing pattern on the input impedance of the tag antenna. This could be done by comparing the measured input impedance of tag antennas, when they are sewed with different kinds of sewing patterns.

REFERENCES

[1] A. Juels, ‘‘RFID security and privacy: a research survey’’, *IEEE Journals on Selected Areas in Communications*, vol. 24, no. 2, pp. 381-394, Feb. 2006.

[2] J. Landt, ‘‘The history of RFID’’, *IEEE Potentials*, vol. 24, no. 4, pp. 8-11, Oct.-Nov. 2005.

[3] P. Salonen, L. Hurme, ‘‘A novel fabric WLAN antenna for wearable applications’’, *IEEE Antennas and Propagation Society International Symposium*, 22-27 June 2003.

[4] P. Salonen, Y. Rahmat-Samii, H. Hurme, M. Kivikoski, ‘‘Effect of conductive material on wearable antenna performance: a case study of WLAN antennas’’, *IEEE Antennas and Propagation Society International Symposium*, 20-25 June 2004, Monterey, California, USA.

[5] P. Salonen, Y. Rahmat-Samii, M. Schaffrath, M. Kivikoski, ‘‘Effect of textile materials on wearable antenna performance: a case study of GPS antennas’’, *IEEE Antennas and Propagation Society International Symposium*, 20-25 June 2004, Monterey, California, USA.

[6] P. Salonen, Y. Rahmat-Samii, M. Kivikoski, ‘‘Wearable antennas in the vicinity of human body’’, *IEEE Antennas and Propagation Society International Symposium*, 20-25 June 2004, Monterey, California, USA.

[7] J. H. Choi, K. Yeonho, L. Kyounghwan, C. C. You, ‘‘Various wearable embroidery RFID tag antenna using electro-thread’’, *IEEE Antennas and Propagation Society International Symposium*, 5-11 July 2008, San Diego, CA, USA.

[8] S. Sankaralingam, B. Gupta, ‘‘Determination of dielectric constant of fabric materials and their use as substrates for design and development of antennas for wearable applications’’, *IEEE Transactions on Instrumentation and Measurement*, vol. 59, no. 12, pp. 3122-3130, Dec. 2010.

[9] K. Yeonho, L. Kyounghwan, K. Yongju, C. C. You, ‘‘Wearable UHF RFID tag antenna design using flexible electro-thread and textile’’, *IEEE Antennas and Propagation Society International Symposium*, 9-15 June 2007, Honolulu, HI, USA.

[10] K. Goojo, L. Jinseong, H. L. Kyoung, C. C. You, Y. Junho, H. M. Byung, Y. Jeenmo, C. K. Hee, ‘‘Design of a UHF RFID fiber tag antenna with electric-

thread using a sewing machine'', *Asia-Pacific Microwave Conference*, 16-20 Dec. 2008, Macau, China.

[11] O. Yuehui, W. J. Chappell, ''High frequency properties of electro-textiles for wearable antenna applications'', *IEEE Transactions of Antennas and Propagation*, vol. 56, no. 2, pp. 381-389, Feb. 2008.

[12] D. M. Pozar, *Microwave engineering*, 2nd edition, John Wiley & Sons, Inc. USA, 1998.

[13] A. Lehto, A. Räisänen, *Radiotekniikan perusteet*, 12th edition, Hakapaino Oy, Helsinki, Finland, 2007.

[14] K. Chang, *Encyclopedia of RF and microwave engineering*, Volumes 1 – 6, John Wiley & Sons, USA, 2005.

[15] D. K. Cheng, *Field and wave electromagnetics*, 2nd edition, Addison-Wesley Publishing Company, Inc. USA, 1992.

[16] D. M. Pozar, *Microwave and RF design of wireless systems*, John Wiley & Sons, USA, 2001.

[17] C. A. Balanis, *Antenna theory - analysis and design*, 3rd edition, John Wiley & Sons, USA, 2005.

[18] S. R. Saunders, A. Aragón-Zavala, *Antennas and propagation for wireless communication systems*, 2nd edition, John Wiley & Sons, USA, 2007.

[19] E. K. Miller, J. A. Landt, ''Direct time-domain techniques for transient radiation and scattering from wires'', *Proceedings of the IEEE*, vol. 68, no. 11, pp. 1396-1423, Nov. 1980.

[20] J.K. Kraus, *Antennas*, McGraw-Hill, New York, 1988.

[21] C. A. Balanis, ''Antenna theory: a review'', *Proceedings of the IEEE*, vol. 80, no. 1, pp. 7-23, Jan. 1992.

[22] C. Capps, ''Near field or far field?'', *EDN*, no. 18, pp. 95-102, 16 Aug. 2001.

[23] W.L. Stutzman, G.A. Thiele, *Antenna theory and design*, 2nd edition, John Wiley & Sons, USA, 1998.

[24] N. Yannopoulou, P. Zimourtopoulos, Wolfram mathematica, Wolfram Demonstrations Project & Contributors, Antennas Research Group [WWW], [accessed on 23.03.2012], available at: http://demonstrations.wolfram.com/DipoleAntennaRadiationPattern/

[25] R.J. Collier, P.D. White, ''Surface waves in microstrip circuits'', *6th European Microwave Conference*, 14-17 Sept. 1976, Rome, Italy.

[26] R. Want, ''An introduction to RFID technology'', *IEEE Parvasive Computing*, vol. 5, no. 1, pp. 25-33, Jan.-March 2006.

[27] L. McCathie, K. Michael, ‘‘The pros and cons of RFID in supply chain management’’, *International Conference on Mobile Business*, July 2005, Sydney, Australia.

[28] B. Zoghi, B. McKee, ‘‘RFID-Based network for personnel and mission-critical asset tracking in a disaster city’’, *38th Annual Frontiers in Education Conference*, 22-25 Oct. 2008, Saratoga Springs, New York, USA.

[29] W. Dong-Liag, W.W.Y. Ng, P.P.K. Chan, D. Hai-Lan, J. Bing-Zhong, D.S. Yeung, ‘‘Access control by RFID and face recognition based on neural network’’, *ICMLC*, 11-14 July 2010, Qingdao, Shandong, China.

[30] C. Hung-Yu, ‘‘Secure access control schemes for RFID systems with anonymity’’, *7th International Conference on Mobile Data Management (MDM)*, 10-12 May 2006, Nara, Japan.

[31] M. Bolić, D. Simplot-Ryl, I. Stojmenović, *RFID systems - research trends and challenges*, John Wiley & Sons, Singapore, 2010.

[32] D.M. Dobkin, *RF in RFID - Passive UHF RFID in practice*, Elsevier, USA, 2008.

[33] P. Pursula, *Analysis and design of UHF and millimeter wave radio frequency identification*, VTT Publications, Helsinki, Finland, 2009.

[34] G. Marracco, ‘‘The Art of UHF RFID antenna design: impedance-matching and size-reduction techniques’’, *IEEE Antennas and Propagation Maganzine*, vol.50, no. 1, pp. 66-79, Feb. 2008.

[35] P. S. Hall, ‘‘Antennas and propagation for body centric communications’’, *First European Conference on Antennas and Propagation*, 6-10 Nov. 2006, Nice, Fance.

[36] J. L. Volakis, Z. Lanlin, W. Zheyu, Y. Bayram, ‘‘Embroidered flexible RF electronics’’, *IEEE International Workshop on Antenna Technology (iWAT)*, 5-7 March 2012, Tucson, Arizona, USA.

[37] L. Zhang, Z. Wang, D. Psychoudakis, J. L. Volakis, ‘‘E-fiber Electronics for body-worn devices’’, *6th European Conference on Antennas and Propagation (EUCAP)*, 26-30 March 2012, Prague, Czech Republic.

[38] Y. Bayram, Z. Yijun, S.S. Bong, X. Shimei, Z. Jian, N.A. Kotov, J.L. Volakis, ‘‘E-textile conductors and polymer composites for conformal lightweight antennas’’, *IEEE Transactions on Antennas and Propagation*, vol. 58, no. 8, pp. 2732-2736, Aug. 2010.

[39] I. Locher, G. Tröster, ‘‘Enabling technologies for electrical circuits on a woven monofilament hybrid fabric’’, *Textile Research Journal*, vol. 78, no. 7, pp. 583-594, July 2008.

[40] W. Zheyu, Z. Lanlin, Y. Bayram, J.L. Volakis, ‘‘Multilayer printing of embroidered RF circuits on polymer composites’’, *IEEE International Symposium on Antennas and Propagation (APSURSI)*, 3-8 July 2011, Spokane, Washington, USA.

[41] W. Zheyu, Z. Lanlin, Y. Bayram, J.L. Volakis, ‘‘Embroidered e-fiber-polymer composites for conformal and load bearing antennas’’, *IEEE International Symposium on Antennas and Propagation (APSURSI)*, 11-17 July 2010, Toronto, Ontario, Canada.

[42] Alien Technology, Morgan Hill, CA, USA. Higgs series tag ICs, available at: http://www.alientechnology.com/tags/rfid_ic.php

[43] Voyantic Ltd, Espoo, Finland, Tagformance lite, available at: www.voyantic.com

[44] Rogers Corporation, RT/duroid 5870/5880/5880LZ High Frequency Laminates, available at: http://www.rogerscorp.com/acm/producttypes/2/Rogers-High-Frequency-Laminates.aspx.

[45] Shieldex, USA, Yarns and fillers, datasheets available at: http://www.shieldextrading.net/yarn_and_filler.html

[46] Y. Ouyang, W. Chappel, ‘‘Measurement of electrotextiles for high frequency applications’’, *IEEE MTT-s International Microwave Symposium Digest*, 12-17 June 2005, Long Beach, CA, USA.